

## Nonlinear fluid flow in random media: Critical phenomena near threshold

Onuttom Narayan

*Physics Department, Harvard University, Cambridge, Massachusetts 02138  
and AT&T Bell Laboratories, 600 Mountain Avenue, Murray Hill, New Jersey 07974*

Daniel S. Fisher

*Physics Department, Harvard University, Cambridge, Massachusetts 02138  
(Received 3 November 1993)*

A simple model for nonlinear collective transport in random media with strong disorder is presented and analyzed. It should apply to systems such as strongly pinned vortex lines in thin superconducting films or low-density fluid flow down a randomly rough inclined plane, in which the randomness is strong enough to break the flow into channels. The model exhibits a threshold force above which macroscopic flow exists. The critical behavior around this threshold is obtained analytically in mean-field theory, which should be valid in three dimensions and higher, and in one dimension. Analytical bounds and numerical simulations are used in the two-dimensional case. Correlation lengths above and below threshold scale differently. Multiple divergent length scales are seen above threshold. Possible modifications due to thermal fluctuations and other effects, and applications to physical systems, are discussed.

### I. INTRODUCTION

Under the influence of an external driving force, collective nonlinear transport occurs in a wide variety of random media: flux lines in superconductors,<sup>1-4</sup> invasion of fluids in porous media,<sup>5-8</sup> sliding charge-density waves<sup>9,10</sup> (CDW's) and various types of electric or mechanical breakdown in inhomogeneous systems.<sup>11</sup> In all of these systems, macroscopic transport occurs in the absence of thermal fluctuations only when the driving force exceeds a threshold magnitude. In the vicinity of the threshold force, the behavior is complicated, involving collective effects over long length and time scales, with correlation lengths that diverge at threshold. These features suggest true critical phenomena near to threshold, and recently the critical behavior near the transition has been analyzed for some of these systems.<sup>10,12</sup>

It is useful to distinguish between two qualitatively different limits for driven collective transport in random media. When the randomness is in some sense weak, the interactions between the transport carriers can produce an elastic structure that, over a wide range of length scales, will distort without breaking.<sup>13</sup> Examples of this class are CDW's,<sup>9,10</sup> weakly pinned Abrikosov flux lattices,<sup>1</sup> single vortex lines,<sup>2,4</sup> fronts of preferentially wetting fluids invading porous media,<sup>5,7</sup> and domain walls in weakly disordered magnets. When, on the other hand, the effects of the randomness are strong, the elastic medium can break up, and the transport becomes much more inhomogeneous and plastic or fluidlike. This is the case, for instance, for strongly pinned vortex lines in the mixed state of superconducting films,<sup>3,4</sup> and for invasion of non-wetting fluids into porous media.<sup>6,7</sup> While driven elastic media have been quite extensively studied, compar-

atively little is known about the fluid or plastic limit. As a first attempt to deal with this regime, we consider a system with no elastic interactions: fluid flow down a rough inclined plane and its generalizations to higher dimensions. We will focus on the critical behavior near to the threshold force of this system, introducing and analyzing a simple model. Specifically, we consider a randomly rough surface onto which fluid is poured, collecting initially into isolated lakes, which we assume do not percolate.<sup>14,15</sup> The surface is now slowly tilted, and fluid spills out of lakes that are full, feeding unfilled lakes further downhill. Above a threshold tilt angle, which is the equivalent of the depinning transition, fluid can flow across an arbitrarily large system from top to bottom. When the tilt is less than its threshold value, there are connected clusters of lakes, as shown in Fig. 1, with all the lakes in a cluster except the one at the terminus full up to the brim. Any further increase in the tilt thus causes fluid to flow from all the lakes in a cluster into the terminus lake. The characteristic size of the clusters increases with the tilt, and diverges at threshold. Above threshold, fluid flows across the entire system, with the current carried in a network of rivers. When the external tilt is much larger than the threshold value, fluid flows over the surface as a sheet, with relatively little spatial structure. On the other hand, near threshold, the flow is extremely inhomogeneous, and is confined to narrow well-separated channels. We shall restrict our analysis in this paper to the behavior near threshold, and shall see that, on both sides of threshold, characteristic length scales diverge as threshold is approached, and thus the transition can indeed be treated as a second-order phase transition. Various features make the analysis of the behavior near threshold difficult. Firstly, there is no simple configuration that can be taken to be a first approxi-

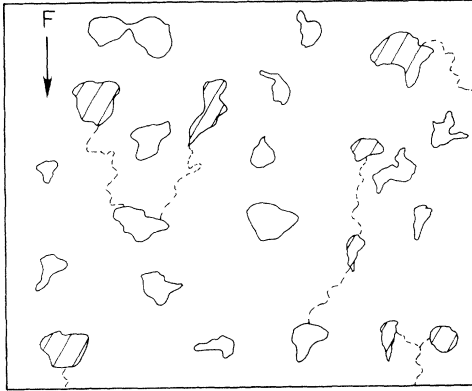


FIG. 1. Schematic of the distribution of fluid on a tilted irregular surface. The direction of the tilt is shown by the arrow. Fluid is located in lakes that are distributed over the surface. Some of these lakes are full to capacity (saturated), and are hatched in this figure. An increase in the tilt force  $F$  causes fluid to flow out of the saturated lakes along the gradient of the surface, and eventually feed into unsaturated lakes. The dashed lines indicate these paths, which have an overall bias in the direction of  $F$ . They connect *clusters* of lakes.

mation, starting from which a perturbative solution can be obtained. Secondly, the transport in this regime is fully nonlinear. Finally, under the influence of gravity, pressure builds up at the terminus of a cluster, rather than being uniform everywhere in it. Thus when the tilt is increased, clusters grow from their terminus sites, with a higher probability of growing if they are already large. This means that one cannot determine the pathways which will dominate the flow above threshold by a *local* analysis that looks for “weak links;” rather, one needs to consider the entire system uphill from a point to determine if current flows through it.

This simple picture approximates the current carriers by a continuous fluidlike medium, instead of discrete objects, and assumes that they are pointlike instead of being extended objects (unlike, for example, flux lines in three-dimensional superconductors). The external force in the model is produced by the tilt, which results in a linearly increasing “gravitational” potential across the system, in contrast, for example, to pressure driven transport. We also assume that the fluid is deposited on the surface initially, rather than “raining” steadily all over the surface, and that the irregularities in the surface are quenched, so that erosion is not allowed for. We shall return to the implications of all these assumptions for the applicability to physical problems later in this paper.

Various models have been considered earlier that somewhat resemble our system either above or below threshold. Below threshold, our system is somewhat like invasion percolation,<sup>16</sup> where fluid is initially distributed on some sites of a lattice, from which it invades other sites by “breaking” bonds connecting them. The external tilt of the surface in our system makes the percolation directed,<sup>17</sup> although the nonlocal nature of the way clusters grow leads to important differences. Above threshold, our system is somewhat similar to various models of

river networks that have been considered recently. However, there are qualitative differences in the structures of the river networks. Our model is also the first that we know of to relate the two sides of the threshold, although, owing to the unusual nature of the transition, the similarities between the two sides are not as extensive as in conventional phase transitions. Comparison with some of the earlier work is discussed later.

The remainder of this paper is organized in the following manner: in Sec. II we discuss in detail the qualitative behavior of the model. This is used to motivate the construction of a simple lattice version of the model, which we use for a quantitative analysis, the results of which are summarized. The behavior of the system as a function of its spatial dimension below and above threshold is obtained in Secs. III and IV, respectively. Comparison with previous work, and modifications due to thermal fluctuations, boundary conditions, and other effects are considered in Sec. V. Finally, possible applications to various physical systems are discussed in Sec. VI. A detailed analysis of the case of one-dimensional systems above threshold is given in Appendix A, Appendix B derives the analytic behavior of the model below threshold, in mean-field theory and in one dimension, and Appendix C analyzes a mean-field approximation above threshold.

## II. QUALITATIVE BEHAVIOR

We first consider the qualitative behavior of the system. As mentioned earlier, fluid is initially distributed randomly over the surface. We take the density of fluid to be below the percolation threshold, so that the fluid is distributed in a series of lakes. If the external tilt  $F$  is slowly increased from zero, the capacity of all the lakes will decrease steadily. Eventually, the capacity of some of the lakes will have decreased sufficiently so as to be just equal to the amount of fluid present in them; these lakes will be saturated, but the barriers at their boundaries prevent the fluid in them from flowing away.

Any further increase in the force  $F$  reduces the capacity of the lakes further. This results in the saturated lakes overflowing by an amount just sufficient to bring them back to saturation. Fluid spills out from these lakes into lakes that are further downhill, which in turn approach saturation. With probability one, there will be a unique direction which is the *lowest* outlet barrier for a given lake to overflow. If the force is increased adiabatically, the path by which fluid overflows from a saturated lake will be over this lowest barrier, and is thus unique.

When  $F$  is increased, fluid overflows from each saturated lake, proceeding downhill, until it pours into some other lake. If this lake is also saturated, it in turn feeds into a lake further downhill; this process continues until an unsaturated lake is reached, where the flow terminates. At any value of  $F$ , it is possible to define “connected clusters” of lakes in the system. Each of these clusters consists of a collection of saturated lakes connected to an unsaturated lake; when  $F$  is increased, fluid spills over from all the saturated lakes in the cluster and, either directly or via other members of the cluster, feeds

into the unsaturated lake, which is the furthest downhill. As  $F$  is increased, more and more fluid flows into the unsaturated lake, which eventually itself reaches saturation. The terminus of the cluster now moves to some unsaturated lake further down, thereby increasing the size of the cluster.

The direction the fluid takes on emerging from a lake is determined by the shape of the surface in the vicinity of the lake. If the irregularities in the surface have only short range correlations, then the direction in which the fluid flows out of widely separated lakes is uncorrelated, except for the overall downhill bias caused by the external force. On long length scales, therefore, the outlet path which goes from one lake to another lower one, and successively downhill, can be taken to be approximately a directed random walk, moving uniformly downhill while executing a random walk in the transverse directions.

Eventually, as  $F$  increases, we expect there to be a cluster spanning the system from top to bottom. Beyond this stage, if  $F$  is increased, fluid flows all the way down the system. If this threshold force  $F_T$  has a well-defined limit as the size of the system is taken to infinity, the transition at  $F_T$  is analogous to a phase transition, with macroscopic transport occurring above the transition. We find that such a transition exists in mean-field theory (and in one dimension), while in two dimensions, numerical simulations support its existence. We thus assume that a well-defined transition occurs in all dimensions.

Above threshold, the total current in the system must in the long time limit be determined by the boundary conditions governing the input of fluid into the system. However, in the limit of an infinite system, it is possible to obtain a solution far from the boundary without reference to the boundary conditions, in terms of only the mean density of fluid in the system. (Strictly speaking, this is a transient solution, which persists in the interior for a time that diverges with the size of the system.) Although most of our analysis will be done using this approach, it is possible alternatively to treat the system as being “current driven,” with fluid being steadily input at the top. We shall discuss this briefly in Sec. V, and also more general issues concerning the effects of boundary conditions.

In order for current to flow across the system above threshold in steady state, there must be rivers carrying fluid connecting the lakes. The depth of fluid in these rivers must be nonzero for them to carry any current. Because of this, there is a finite probability for a river to split into two. In addition, for current to flow through a lake, the depth of fluid has to be greater than the lowest outlet barrier of the lake, so that fluid may be able to spill out of a lake in more than one direction. Thus unlike the case below threshold, where the fluid overflows from saturated lakes along unique paths, the transport paths branch above threshold. This branching process is balanced by rivers colliding into each other and joining as they proceed downhill. Far from the top of the system, an equilibrium density of rivers is established, and there is a connected network of rivers through which the steady state flow takes place.

### A. Critical behavior

It is possible to define correlation lengths both above and below threshold as suitable characteristic length scales associated with the system. The external force  $F$  singles out a particular direction; thus there are different correlation lengths,  $\xi \equiv \xi_{\parallel}$  and  $\xi_{\perp}$ , parallel and perpendicular to the direction of the tilt. Below threshold, the correlation lengths can be chosen to be the characteristic size of the large connected clusters, which diverge at threshold.<sup>18</sup> Above threshold, the length scales above which the coarse grained current is approximately homogeneous yield natural correlation lengths.<sup>19</sup> Far above threshold, when the flow is large, the current is fairly uniform, while close to threshold there are widely spaced rivers that drain only a small fraction  $\phi$  of the system, the rest being in isolated clusters of lakes that are not connected to the river system. Thus the correlation lengths diverge as threshold is approached from above, associated with the low density of the river network, while below threshold they diverge with the diverging characteristic cluster size. We thus have behavior similar to that found in conventional critical phenomena, in particular, for percolation.<sup>14,15</sup> We conjecture that the correlation lengths,  $\phi$ , and other quantities scale as powers of the reduced force,

$$f \equiv F/F_T - 1, \quad (2.1)$$

close to threshold. Thus we conjecture that the mean current density flowing through the system just above threshold has the form

$$\bar{J} \sim f^{\beta}, \quad (2.2)$$

where we have introduced an exponent  $\beta$  analogous to that for CDW's.<sup>10,20</sup>

It is useful to generalize the river flow problem from two dimensions to  $d$  dimensions, with one downhill direction and  $d - 1$  transverse directions. When  $d = 1$ , the number of transverse directions is zero, so that it is no longer meaningful to talk about flow patterns across the system; the entire system has current flowing through it above threshold, and  $\phi = 1$ . Nevertheless, distances in the direction of the applied force are still well defined, so that  $\xi$  exists. We shall introduce a lattice model to analyze the case of  $d > 1$ , but since the flow pattern in higher dimensions is locally one dimensional in rivers and near to the outlets of lakes, it is instructive to consider the one-dimensional continuum behavior first, as a guideline towards constructing this lattice model.

Figure 2 illustrates the pattern in which fluid is distributed in the one-dimensional system, showing lakes of varying sizes. The details of the behavior are discussed in Appendix A; here the relevant results are summarized. It is first shown that there is a well-defined threshold force  $F_T$ . Above this force, all the lakes are connected sequentially by a series of rivers. The depth of these rivers tends to zero as threshold is approached from above. Above threshold, it is useful to define the concept of “excess fluid,” which is the amount of fluid per unit length of the

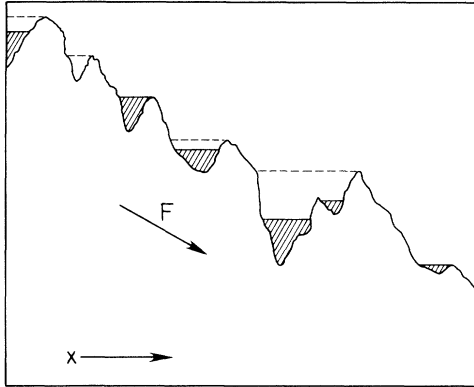


FIG. 2. Schematic of the one-dimensional system. The arrow indicates the direction of the tilt produced by the external force  $F$ . The lakes are the hatched regions in the figure. The dashed lines denote the capacity of the lakes that are unsaturated. They are constructed by proceeding backwards from the downhill (right) end of the system.

system that it would be necessary to remove in order to bring the system back to threshold. Because the capacity of the lakes decreases smoothly with  $F$ , the excess fluid scales linearly with  $f$  close to threshold. As threshold is approached, more and more of this excess fluid is present in the lakes, rather than in the rivers. As shown in Appendix A, this results in the current flowing out of the lakes near threshold being independent of time, so that steady state solutions are applicable.<sup>21</sup> The current flowing through the system is dominated by the behavior near the outlet “lip” of each lake, which is the barrier over which it overflows. The fluid flow is essentially a function of the height of fluid above the barrier at this lip. (This of course does not mean that only the fluid above the barrier at any site participates in the flow, but rather that the flow rate can be expressed simply as a function of this difference.)

### B. Lattice model

We now introduce a simple lattice model for  $d > 1$ . It has sites distributed on a hypercubic lattice; each site represents a lake in the original continuum system. The pathways along which rivers are allowed to flow are modeled by bonds that connect any site to all its nearest neighbors. The force  $F$  is imposed in the downhill  $111\dots$  direction of the lattice. There are  $(d-1)$  directions transverse to this force. As discussed earlier, in the continuum system the rivers flow downhill on long length scales. It therefore suffices in the lattice version for each site  $i$  to have outlets connecting it only to its  $d$  nearest neighbors  $i_\alpha$  in the next hyperplane downhill. An illustration of the model is shown in Fig. 3. Motivated by the one-dimensional behavior discussed above, we take the current flowing in a river to depend only on the depth above the lip of the lake it emerges from. Accordingly, a barrier  $b_{i\alpha}$  is assigned to each outlet  $\alpha$  emerging from a site  $i$ ; this barrier controls the current flowing through the outlet. These barriers are taken randomly from a

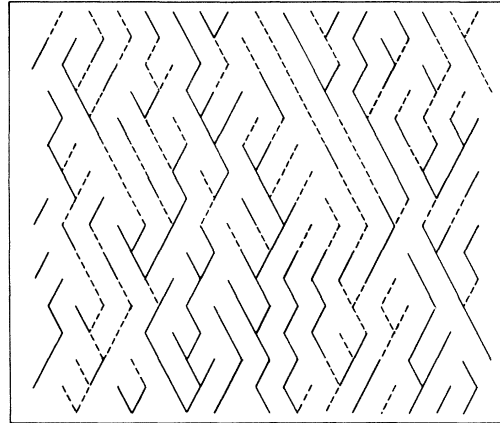


FIG. 3. Typical outlet tree in the lattice model in two dimensions, formed by considering the path emerging from each site that has the lowest barrier associated with it. The solid lines are the clusters, which are subsets of the outlet tree; all the sites in a cluster except the lowest one are saturated. The size of the large characteristic clusters grows with  $F$ , and diverges at threshold.

distribution  $B(b)$ , and are chosen independently, since correlations in the continuum landscape are assumed to be short ranged. At each site  $i$  of the lattice, there is a depth of fluid  $h_i$ . Based on the one-dimensional behavior, we take the current  $J_{i\alpha}$  flowing through an outlet  $\alpha$  from a site  $i$  to be

$$J_{i\alpha} = 0 \text{ if } h_i < b_{i\alpha} - F$$

and (2.3)

$$J_{i\alpha} = (h_i - b_{i\alpha} + F)^{\beta_0} \text{ if } h_i > b_{i\alpha} - F.$$

The exponent  $\beta_0$  characterizes the flow over the barrier lip, and will affect the macroscopic dynamics in a similar way to the effect of geometrical constrictions on the conductivity near continuum percolation.<sup>22</sup> For fluid flow in a smooth potential,  $\beta_0$  can be obtained from the one-dimensional analysis of Appendix A, and the natural choice is  $\beta_0 = 3 + d/2$ . Because an increase in the driving force near threshold is equivalent to a proportional increase in the excess fluid in the system, the dependence on  $F$  in Eq. (2.3) occurs only through the variable  $h_i - F$ . Alternatively, an increase in  $F$  is equivalent to lowering all the barriers  $b_{i\alpha}$  uniformly.

In the continuum system we wish to model, the lakes are neither distributed in a regular array, nor are they connected only to nearest neighbors. Nevertheless, even in the continuum system the connections produced by the rivers are primarily only short ranged; we therefore expect that the behavior at long distances should be the same as for the lattice model used here.

### C. Summary of results

We now briefly summarize some of the main results. The lattice model defined above can be solved below

threshold in mean-field theory. The correlation length exponent, defined through  $\xi \equiv \xi_{\parallel} \sim |f|^{-\nu}$  is found in mean-field theory to be

$$\nu = \frac{3}{2}. \quad (2.4)$$

The transverse correlation length,  $\xi_{\perp}$ , scales as  $\sim \sqrt{\xi}$  in all dimensions. The mass  $s$  of a cluster, i.e., the total number of sites in it, scales with the downhill length  $l$  of the cluster as

$$s \sim l^{d_f}, \quad (2.5)$$

with the mean-field value of the ‘‘fractal dimension’’  $d_f$  found to be

$$d_f = \frac{4}{3}. \quad (2.6)$$

The fraction of sites which are in clusters of length  $\sim \xi$  scales as  $\xi^{-\kappa}$ , with

$$\kappa = \frac{2}{3} \quad (2.7)$$

in mean-field theory. The polarization density, defined as the mean distance moved by a drop of fluid from its initial position at  $F = 0$ , has a singular part that scales as

$$\Pi_s \sim |f|^{1-\gamma} \quad (2.8)$$

with

$$\gamma = \nu(1 - \kappa). \quad (2.9)$$

From Eqs. (2.7) and (2.4), in mean-field theory  $\gamma$  is given by

$$\gamma = \frac{1}{2}, \quad (2.10)$$

a result that can be derived directly.

Above threshold, one can define the parallel correlation length  $\xi'$  as the typical downhill distance over which the current is correlated; this scales as  $\xi' \sim f^{-\nu'}$ . The fraction of sites that feed fluid into the rivers scales as

$$\phi \sim f^{\Gamma}. \quad (2.11)$$

By matching the behavior at threshold with the scaling forms above and below threshold, we obtain

$$\Gamma = \kappa\nu'. \quad (2.12)$$

The exponents  $\Gamma$  and  $\nu'$  can also be related by considering the characteristic downhill interval between two splits of a river;  $\Gamma$  determines the amount of fluid flowing in the rivers, which is in turn related to the probability of a river splitting. In mean-field theory, we derive the relation

$$\nu' = \frac{1 + \Gamma}{2}. \quad (2.13)$$

Combining Eqs. (2.12) and (2.13) with Eq. (2.7), we obtain

$$\nu' = \frac{3}{4} \quad (2.14)$$

and

$$\Gamma = \frac{1}{2}, \quad (2.15)$$

therefore yielding  $\nu \neq \nu'$ , a rather surprising result. The current exponent,  $\beta$ , is found to obey the relation

$$\beta = \left[ \frac{1 + \Gamma}{2} \right] (1 + \beta_0) \quad (2.16)$$

and thus depends on the ‘‘microscopic’’ local exponent  $\beta_0$ .

The upper critical dimension, above which the mean-field solution is valid, is argued from the properties of random walks to be three. In less than three dimensions, the critical exponents are modified from their mean-field values. However, Eqs. (2.9), (2.12), and (2.16), which express relations between the exponents, are still valid. Equation (2.13) is modified to

$$\nu' = \frac{1 + \Gamma}{d - 1} \quad (2.17)$$

which agrees with Eq. (2.13) at the upper critical dimension,  $d = 3$ . An *extra* relation between the exponents, that is not valid in mean-field theory, is also obtained:

$$\kappa + d_f = \frac{d + 1}{2}, \quad (2.18)$$

based on arguments analogous to hyperscaling in conventional phase transitions. (This equation is satisfied by the mean-field exponents at  $d = 3$ .) All the principal exponents are thus expressed for  $d < 3$  in terms of  $\kappa$  and  $\nu$ , with those above threshold depending only on  $\kappa$ . In two dimensions, through numerical simulations of the behavior below threshold, we obtain the estimates

$$\kappa = 0.29 \pm 0.02, \quad (2.19)$$

implying, from Eq. (2.18),

$$d_f = 1.21 \pm 0.02 \quad (2.20)$$

and

$$\nu = 1.76 \pm 0.02. \quad (2.21)$$

For the special case of  $d = 1$ , it is also possible to solve for the behavior below threshold analytically. Since the length of a cluster is now equal to the number of sites in it,  $d_f = 1$  trivially. Also, since above threshold there is a single river flowing from top to bottom of the system, and river splits are not possible,  $\Gamma = 0$ , and  $\nu'$  is not defined. The nontrivial exponents are found to be

$$\kappa = 0, \quad \nu = 2, \quad \text{and} \quad \gamma = 2, \quad (2.22)$$

satisfying Eq. (2.9). Equation (2.16) is altered, because of the absence of river splits; in fact, in one dimension,  $\beta = \beta_0$ .

### III. BELOW THRESHOLD

In this section, we analyze the critical behavior below threshold of the lattice model constructed in the previous section. By assuming a scaling form for the distribution of clusters of different sizes, it is possible to relate the various critical exponents. This scaling conjecture is verified analytically in mean-field theory and for  $d = 1$ , and is consistent with numerical simulations in two dimensions.

#### A. Scaling of clusters

Below threshold, there are no steady state currents, and, after initial transients have decayed away,  $h_i + F \leq \min_{\alpha} b_{i\alpha}$  for all sites, with the equality being satisfied at saturated sites. Thus only the lowest barrier associated with any site is significant. Figure 3 shows a typical realization of the lattice, where for all the sites only the outlets with the lowest barriers are shown. Each site has a unique outlet path leading downhill, which is determined by following the sequence of lowest barriers going downwards from the site. All the sites are thus connected in a tree. As  $F$  is increased, a saturated lake will spill excess fluid into the unique lake connected to it on the next row down in the outlet tree. Subsections of the outlet tree form connected clusters of saturated lakes, with an unsaturated lake at the terminus of each. Because the full outlet path from any site is determined by independent events, these paths are random walks in the  $d - 1$  transverse directions, so that clusters of length  $l$  in the downhill direction typically have a width  $w \sim l^{1/2}$  in the transverse directions. By analogy with percolation,<sup>14,15,17</sup> we expect the probability of large clusters to fall off exponentially with a characteristic length  $\xi$ —and corresponding width  $\xi_{\perp} \sim \xi^{1/2}$ —defining the correlation lengths. The mass  $s$  of a cluster, which is the number of sites it contains, can be used to define a fractal dimension, through  $s \sim l^{d_f}$ . Note that we have chosen to scale with downhill lengths in defining  $d_f$ .

By analogy with percolation,<sup>14,15</sup> we conjecture a scaling form for the probability of a site being in a cluster of length  $l$ :

$$\rho(l, F) dl = l^{-\kappa} \hat{\rho}(l/\xi) \frac{dl}{l} \quad (3.1)$$

for large  $l$  and  $\xi$ , with  $\xi$  diverging at  $F_T$  as  $\xi \sim |f|^{-\nu}$ . (The length  $l$  is actually restricted to integer values; the factor of  $dl$  is introduced for convenience in calculating scaling properties, for which the continuum approximation is a good one.) The fraction of the volume filled by clusters of length of order  $\xi$  is thus  $\xi^{-\kappa} \sim |f|^{\kappa\nu}$ .

#### B. Polarization

The mean distance that a drop of fluid has moved from its initial position can be used to define a mean polarization density  $\Pi$ , whose singular part we conjecture behaves as  $\Pi_s \sim |f|^{-\gamma+1}$  near threshold. It is possible to extract

$\gamma$  from a scaling argument: Consider a cluster of length  $\xi$ . If the distance to threshold is decreased from  $f$  to  $f/2$ , this is equivalent to adding an amount of fluid  $f/2$  to each site. On any cluster of size  $\xi$ , all the additional fluid drains immediately to the terminus of the cluster, thereby moving a typical distance  $\sim \xi$ . Since the fraction of sites that are in clusters of length  $\sim \xi$  is  $\sim \xi^{-\kappa}$ , the amount of fluid that moves down because of the increase in  $F$  is  $\sim \xi^{-\kappa} |f|/2$ . Some of the clusters will increase in length due to the reduction in  $|f|$ , and fluid from them will flow out beyond their terminus sites. But since  $\xi$  will only increase by a factor of  $2^{\nu}$ , this fluid will typically go a distance which is not more than a few times  $\xi$ . There is also an increase in polarization from smaller clusters that become connected to the size  $\xi$  cluster. Again, since such connections result in an increase in the total size of the original cluster, by an amount which is typically not more than some multiple of its original size, this will only change the polarization estimated from isolated clusters by a numerical factor. There are also less singular contributions to the polarization from displacement across smaller clusters, with size  $\ll \xi$ . Thus we expect that it is only the *singular* part of the polarization density which is dominated by cluster lengths  $\sim \xi$ ; these yield  $\delta\Pi_s \sim \xi^{1-\kappa-1/\nu}$ , from which, using the definition of  $\gamma$ ,  $\Pi_s \sim |f|^{-\gamma+1}$ , we obtain

$$\gamma = \nu(1 - \kappa). \quad (3.2)$$

This is similar to a standard scaling argument in percolation,<sup>14</sup> which relates the susceptibility to the typical mass and number of connected clusters, although here the relevant quantity is the length of a cluster, instead of its mass.

For the case of  $\gamma = 1$ , in the scaling argument we have constructed,  $\delta\Pi_s \sim \xi^{(\gamma-1)/\nu} \sim \text{const}$ . Since  $\delta f = -f/2$ , the polarizability  $\chi_s = d\Pi_s/df \sim 1/|f|$ , from which  $\Pi_s \sim \ln(1/|f|)$ . However, when  $\gamma = 0$ ,  $\delta\Pi_s \sim |f|$ , so that  $\chi_s \sim \text{const}$  rather than having a logarithmic divergence.

#### C. Mean-field theory

As mentioned earlier, it is possible to solve for the behavior below threshold in a mean-field limit, verifying the scaling form conjectured in Eq. (3.1), as well as obtaining all the critical exponents. The details of the solution are given in Appendix B; here the main features are outlined.

We define a quantity  $a_i$  at every site  $i$  in the lattice, as the *initial* value of  $h_i + F - \min_{\alpha} b_{i\alpha}$ , before the lattice equilibrates by fluid flowing out of overfull sites. (Below threshold, the *equilibrium* value of this quantity cannot be positive for any site  $i$ .) The  $a_i$ 's are thus chosen independently for all the sites, from the same distribution  $A(a)$ , which is related simply to  $B(b)$ . We also define a quantity  $\Delta_i$ , as the value of  $h_i + F - \min_{\alpha} b_{i\alpha}$  in a site  $i$  *after* all the sites in the rows above it have been equilibrated, but *before* the site  $i$  has overflowed down to the next row (which will happen when  $\Delta_i > 0$ ). If  $i_1, \dots, i_r$  are the “inlets” to the site  $i$ , i.e., the sites that are in the row immediately preceding  $i$  and linked to it through the outlet tree of Fig. 3, any site  $i_k$  for which  $\Delta_{i_k} > 0$  spills an amount  $\Delta_{i_k}$  of fluid into the site  $i$ . Thus

$$\Delta_i = a_i + \sum_{k=1}^r \max[\Delta_{i_k}, 0]. \quad (3.3)$$

The inlets to a site  $i$  are denoted with roman subscripts,  $i_k$ , while the outlets are denoted as  $i_\alpha$ . For finite dimensionality  $d$ , the number of inlets of two neighboring sites in the same row are anticorrelated. For instance, for  $d = 2$ , if a site  $i$  has two inlets, neither of its adjacent sites can have more than one inlet. There are two special cases when this anticorrelation does not exist, and the problem can be cast in terms of independent probability distributions  $\tilde{P}(\Delta)$  for all the sites in the same row. The first is for  $d = 1$ , when every site has exactly one inlet. The second is in a mean-field limit, where the correlations in the number of inlets and the amount of fluid input from them are ignored; this should be valid in the limit of large  $d$ . The mean-field limit can also be obtained by considering long range (transverse to the downhill direction) outlet connections between sites, which will yield independent inputs. We now analyze such a mean-field limit, where the  $\Delta_{i_k}$  are *independent*.

If  $c_r$  is the probability that a site has  $r$  inlets, the distribution  $\tilde{P}_{m+1}(\Delta)$  of  $\Delta$  for sites in the  $(m+1)$ th row from the top is given in terms of  $\tilde{P}_m(\Delta)$  by

$$\begin{aligned} \tilde{P}_{m+1}(\Delta) &= \sum_{r=0}^{\infty} c_r \prod_{j=1}^r \left[ \int_0^{\infty} d\Delta_j \tilde{P}_m(\Delta_j) \right] \\ &\times A\left(\Delta - \sum_j \Delta_j\right). \end{aligned} \quad (3.4)$$

The initial condition on the top row in Eq. (3.4) is  $\tilde{P}_0(\Delta) = A(\Delta)$ . The probabilities  $c_r$  satisfy the constraints  $\sum c_r = 1$  and  $\sum r c_r = 1$ , where the second equation follows from the fact that each site has one outlet. The case of  $d = 1$  can be treated as a special case of Eq. (3.4), with  $c_r = \delta_{r,1}$ . One might hope that any set of probabilities which allow multiple inputs, i.e.,  $c_r \neq 0$  for some  $r > 1$ , will behave similarly. Most of the mean-field analysis in Appendix B is restricted to the case  $c_0 = c_2 = \frac{1}{4}$ ,  $c_1 = \frac{1}{2}$ , for which it is possible to solve Eq. (3.4) explicitly for certain distributions  $A(a)$ , but other choices for the  $c_r$ 's are argued to yield the same behavior.

Below threshold, one expects to find a fixed point  $\tilde{P}(\Delta)$  to which the solution  $\tilde{P}_m(\Delta)$  of Eq. (3.4) converges for large  $m$ . Threshold occurs at the value of  $F$  for which this fixed point distribution disappears; for larger  $F$ , the typical amount of fluid present in the lowest row of a lattice of length  $L$  diverges with  $L$ . No meaningful information can be extracted for the behavior above threshold by the method of row by row equilibration used here; the state above threshold is a nonequilibrium one, where steady

state is only established because it takes time for fluid to move downhill.

It is useful to consider the modified probability distributions,

$$P_m(\Delta) = \theta(\Delta) \tilde{P}_m(\Delta) + \delta(\Delta) - \int_{-\infty}^0 d\Delta' \tilde{P}_m(\Delta') \quad (3.5)$$

for the amount of *overflow*, i.e.,  $\max[\Delta, 0]$ . Since the only sites in the  $m$ th row that contribute to the  $(m+1)$ th row are those for which  $\Delta > 0$ , this modification does not affect the evolution. Since Eq. (3.4) generates  $\tilde{P}_{m+1}$ , rather than  $P_{m+1}$ , in order to obtain the evolution equation for  $P$ , one has to add an extra term to the right-hand side that shifts all the weight of  $\tilde{P}_{m+1}(\Delta)$  at  $\Delta < 0$  to  $\Delta = 0$ . We thus obtain

$$\begin{aligned} P_{m+1}(\Delta) &= \sum_{r=0}^{\infty} c_r \prod_{j=1}^r \left[ \int_0^{\infty} d\Delta_j P_m(\Delta_j) \right] A\left(\Delta - \sum_j \Delta_j\right) \\ &- \hat{\mu}_m(\Delta) + \delta(\Delta) \int_{-\infty}^0 d\Delta' \hat{\mu}_m(\Delta') \end{aligned} \quad (3.6)$$

where the integrals of  $\Delta_j$  include the  $\delta$  function at  $\Delta_j = 0$ . The function  $\hat{\mu}_m(\Delta)$  is  $\theta(-\Delta) \tilde{P}_{m+1}(\Delta)$ , but in Appendix B we find that it is convenient to treat it as a function to be determined self-consistently:  $\hat{\mu}_m$  only has support for  $\Delta < 0$ , and must yield a  $P_{m+1}$  which is zero for  $\Delta < 0$ . In terms of the Fourier transforms of the distributions,  $P_m(\omega) = \int_{-\infty}^{\infty} d\Delta P_m(\Delta) \exp[i\omega\Delta]$  [and likewise for  $\hat{\mu}(\Delta)$  and  $A(\Delta)$ ], Eq. (3.6) becomes<sup>23</sup>

$$P_{m+1}(\omega) = \sum_{r=0}^{\infty} c_r A(\omega) [P_m(\omega)]^r + \hat{\mu}_m(\omega = 0) - \hat{\mu}_m(\omega). \quad (3.7)$$

To obtain the distribution of cluster masses, it is necessary to keep track of the number of sites  $s_i$  that the output of a site  $i$  adds to the cluster to which it might overflow. This is zero if the site does not overflow, i.e., if  $\Delta_i < 0$ . If  $\Delta_i > 0$ ,  $s_i$  is one more (the site  $i$  itself) than the total number of sites connected to  $i$  from above by overflow. Thus

$$s_i = 1 + \sum_k s_{i_k} \quad \text{for } \Delta_i \geq 0$$

and

$$s_i = 0 \quad \text{for } \Delta_i < 0 \quad (3.8)$$

with the sum running over all the inlet sites  $i_k$  for the site  $i$ . We now define a joint distribution, at the  $m$ th row, of  $\max[\Delta, 0]$  and  $s$ :  $P_m(\Delta; s)$ . This obeys the recursion relation

$$\begin{aligned} P_{m+1}(\Delta; s) &= \sum_{r=0}^{\infty} c_r \prod_{j=1}^r \left[ \int d\Delta_j \sum_{s_j} P_m(\Delta_j; s_j) \right] A\left(\Delta - \sum_j \Delta_j\right) \delta_{s, 1 + \sum s_j} \\ &- \hat{\mu}_m(\Delta; s) + \delta_{s,0} \delta(\Delta) \sum_{s'=1}^{\infty} \int_{-\infty}^0 d\Delta' \hat{\mu}_m(\Delta'; s'), \end{aligned} \quad (3.9)$$

where the function  $\hat{\mu}_m(\Delta; s)$  cancels the first term for  $\Delta < 0$  and each  $s$ , and the last term replaces this weight with a  $\delta$  function at  $\Delta = s = 0$ , corresponding to sites that do not overflow. The function  $\hat{\mu}_m(\Delta; s)$  has support only for  $\Delta < 0$  and vanishes for  $s = 0$ : it is thus the probability that a site connected to  $s - 1$  sites above it does not overflow and has  $\Delta < 0$ . The integral

$$\mu_m(s) = \int d\Delta \hat{\mu}_m(\Delta; s) \quad (3.10)$$

is thus the probability that a site in the  $(m - 1)$ th row down from the top of the system is the terminus of a cluster of mass (including the site itself)  $s$ , and therefore yields the distribution of cluster masses.

As shown in Appendix B, for the special case when  $A(a) \propto \exp[a]$  (or some other simple exponential) for  $a < 0$ ,  $\hat{\mu}_m(\Delta; s)$  is of the form  $\mu_m(s) \exp[\Delta] \theta(-\Delta)$ . With the expectation that the critical behavior should be independent of the precise form of  $A(a)$  [except perhaps when  $A(a)$  has long power-law tails], we analyze the behavior for this case. In the same spirit, we choose a specific form for  $A(a)$ :

$$\begin{aligned} A(a) &= \exp[-a/g]/(1+g) \quad \text{for } a > 0 \\ &= \exp[a]/(1+g) \quad \text{for } a < 0 \end{aligned} \quad (3.11)$$

so that  $A$  is continuous. Since  $a_i = h_i + F - \min_\alpha b_{i\alpha}$ , an increase in  $F$  really corresponds to shifting the whole distribution  $A(a)$  to the right:  $A'(a) = A(a - \delta F)$ . Thus instead of Eq. (3.11), one should consider the distribution

$$A(a) = \theta(F - a) \exp[a - F] \quad (3.12)$$

as a function of  $F$ . This distribution, although simpler in form, leads to mean-field equations that cannot be solved easily, unlike Eq. (3.11), from which various properties, including scaling functions, are obtained explicitly in Appendix B. The critical behavior for both distributions is controlled by the *low frequency* forms of their Fourier transforms, which are equivalent. We therefore work with the distribution in Eq. (3.11). The parameter  $g$  controls the distance to threshold. Increasing  $g$  increases the weight of  $A(a)$  for  $a > 0$ , thereby driving the system towards threshold. By considering the low frequency forms of  $A(\omega)$  obtained from Eqs. (3.11) and (3.12), we see that  $g_T - g \propto F_T - F$ .

Below threshold, far from the top of the system, all the probability distributions should converge to fixed point forms independent of  $m$ . We thus define fixed point distributions and transforms

$$P(\omega; y) = \sum_{s=0}^{\infty} y^s P(\omega; s), \quad (3.13)$$

so that  $P(\omega; y = 1) = P(\omega)$ , and likewise for  $\mu$ . For the special case with  $A(a) \propto e^a$  for  $a < 0$ , Eq. (3.9) then yields

$$P(\omega; y) = \sum_{r=0}^{\infty} c_r y A(\omega) [P(\omega; y)]^r + \mu(y = 1) - \frac{\mu(y)}{1 + i\omega}. \quad (3.14)$$

The function  $\mu(y)$  has to satisfy the normalization condition,  $d\mu(y)/dy|_{y=1} = 1$ , since the probability of a site being in a cluster of size  $s$  is  $s\mu(s)$ , so that  $\sum s\mu(s) = 1$ ;  $\mu(y = 1)$  is thus the total number density of clusters.

For the simple case when  $c_r = 0$  for  $r > 2$ , Eq. (3.14) is a quadratic in  $P(\omega; y)$ , which can be formally solved to obtain  $P$  in terms of  $\mu$ . (The general case without this restriction is discussed briefly in Appendix B.) The condition that  $P(\Delta; s)$  is a probability distribution with no support for  $\Delta < 0$  is sufficient to determine  $\mu(y)$ , as is done in Appendix B. The only singularity in  $\mu(y)$  is a branch cut of the form  $\sim [(1-2g)^2 + (3g^2 - 6g)(1-y)]^{3/2}$ . The branch cut moves in to  $y = 1$  at  $g = g_T = 1/2$ , giving rise to power-law distributions for  $\mu(s)$ . Near the critical point,  $g = 1/2 - \epsilon$ , the scaling form of  $\mu(s)$  is obtained from contour integration around the singularity in  $\mu(y)$  to be

$$\mu(s) \sim \frac{1}{s^{5/2}} \exp[-16\epsilon^2 s/9] \quad (3.15)$$

with  $\epsilon \equiv g_T - g = \frac{1}{2} - g$  small and  $s$  large, but any value of the scaling variable  $\epsilon^2 s$ . Since the probability of being in a cluster of size  $s$  scales as  $s\mu(s)$ , and  $s \sim l^{d_f}$ , we thus obtain

$$\frac{\kappa}{d_f} = \frac{1}{2} \quad (3.16)$$

and

$$d_f \nu = 2. \quad (3.17)$$

The scaling of the singular part of the polarization can be obtained directly from the asymptotic form of  $P(\Delta)$  for large  $\Delta$ . An increase in  $F$  results in fluid being displaced downhill; far from the top of a system, below threshold, the amount of fluid that flows out of any row into the next is independent of the row considered. In the limit of infinite system size, when the depletion layer near the top can be ignored, the polarization density in the bulk is equal to the mean amount of fluid that pours out of the lowest row of the lattice, at the bottom of the system, which is just the first moment of  $P_m(\Delta)$  for the bottom row. Thus the mean value of  $\Delta$  for the fixed point distribution  $P(\Delta)$  is equal to the singular part of the polarization density. Setting  $y = 1$  in Eq. (3.14), and using the calculated value for  $\mu(y = 1)$ , we solve for  $P(\omega)$ . The singular part of the polarization is  $\int d\Delta [\Delta P(\Delta)]$ , which is  $-idP(\omega)/d\omega|_{\omega=0}$ . From Eq. (B32), this is seen to scale as  $\Pi_s \sim \epsilon^{1/2}$ , so that

$$\gamma = 1/2. \quad (3.18)$$

The correlation length can be found by adding a small perturbation  $\delta P(\Delta)$  to the fixed point distribution,  $P(\Delta)$ . From the distance downhill it requires for the effect of the perturbation to decay away, the scaling of the correlation length can be found. In Appendix B, we obtain

$$\nu = 3/2 \quad (3.19)$$

which, when combined with Eqs. (3.16) and (3.17), yields

$\kappa = 2/3$  and  $d_f = 4/3$ , as in Eqs. (2.6) and (2.7). As a consistency check, these exponents can be substituted in Eq. (3.2), yielding  $\gamma = 1/2$ , as in Eq. (3.18).

It is possible to obtain an inequality,  $\kappa + d_f \geq 2$ , for the mean-field exponents, from the requirement that separate clusters must by definition not collide with each other. Since each cluster is a subset of the outlet tree of Fig. 3, the mean number of clusters that exist in a system of length  $\xi$  can be found by starting a set of random walks at the top of the system, and asking how many of them survive for a distance  $\sim \xi$  downhill. The number of random walks that survive for a downhill distance of  $l$  decreases with  $l$  because of two reasons. First, some of the walks terminate “spontaneously” at each row, corresponding to clusters terminating upon reaching an unsaturated site. Second, when two random walks meet, they join together, thereby decreasing the total number of walkers. If the first of these two factors is ignored, an upper bound is obtained on the number of clusters that survive for a distance  $\xi$ . In mean field, where each site is linked in the outlet tree to a random site in the next row, when only mutual intersections are allowed to decrease the number of walkers, the density of distinct random walks  $\sigma(l)$  that survive for a length  $l$  decays as  $d\sigma/dl \sim -\sigma^2$ . This implies an asymptotic form  $\sigma(l) \sim 1/l$ . Since  $\xi_{\perp} \sim \xi^{1/2}$ , the number of clusters of length  $\sim \xi$  in a correlation volume is therefore  $n(\xi) \leq O(\xi^{\frac{d-1}{2}}/\xi)$  in mean field. On the other hand, since the fraction of the volume occupied by these clusters scales as  $\xi^{-\kappa}$ , by the definition of  $\kappa$ ,

$$n(\xi) \sim \xi^{\frac{d+1}{2} - \kappa - d_f} \quad (3.20)$$

in any dimension. Comparing these two forms yields  $\kappa + d_f \geq 2$  in mean field. This inequality is in fact saturated by the mean-field exponents obtained earlier.

#### D. Upper critical dimension

The picture of clusters arising from independent random walks can be used to guess the upper critical dimension,  $d_c$ , above which mean-field theory is exact asymptotically. The clusters perform random walks in the  $(d-1)$ -dimensional transverse space, with the downhill direction acting as the time coordinate. For  $d-1 > 2$ , two walks that start out close to each other have a finite probability of not colliding for an arbitrarily long time. (There are logarithmic corrections for  $d-1 = 2$ .) On the other hand, for  $d-1 < 2$ , the probability of the two walks never colliding vanishes. The correlations in the positions of the walks, which arise from the fact that they get sparser as one proceeds down the system, thus become important in determining collision probabilities, and the simple arguments in the previous paragraph will no longer apply. On the other hand, the long distance behavior for all  $d-1 > 2$  should be essentially similar, which suggests that  $d_c$  should be 3.

In the absence of a full renormalization group treatment of the problem, it is not possible to obtain the upper critical dimension rigorously. However, scaling consider-

ations can be used to estimate the importance of region to region variations; by defining the upper critical dimension as the value of  $d$  below which such variations are important, we find  $d_c = 3$ , in agreement with our arguments above. If mean-field values are used in Eq. (3.20) for the exponents, the number of clusters in a correlation volume is  $n(\xi) \sim \xi^{(d-3)/2}$ . For  $d > 3$ , there are a large number of intertwined characteristic large clusters (i.e., with length  $\sim \xi$ ) in a correlation volume. For  $d < 3$ , the mean-field expression must break down. The variations in the number of clusters from region to region can no longer be ignored, and the exponents are changed from their mean-field values. As in conventional critical phenomena and percolation, scale invariance is expected below the upper critical dimension (if lengths are scaled by the correlation lengths), so that for  $d < 3$ , there will be  $O(1)$  characteristic clusters in a correlation volume. (This expectation will be verified in Sec. IV.) From Eq. (3.20),

$$d_f = \frac{d+1}{2} - \kappa \quad (3.21)$$

for all  $d < 3$ . At the upper critical dimension,  $d = 3$ , this equation is satisfied by the mean-field exponents. (The exponents for  $d = 1$  also satisfy this equation.) Equation (3.21) implies that the region to region variations in the number of clusters in a correlation volume scales in the same way as the number of clusters; this is the equivalent of the hyperscaling relation,  $d\nu = 2 - \alpha$ , which is valid for conventional percolation.<sup>14,15,17</sup> Thus, below  $d_c = 3$ , only two independent exponents are expected below threshold. At the critical dimension,  $d = 3$ , there are likely to be logarithmic corrections to some or all of the exponents.

#### E. One-dimensional case

The one-dimensional case, when  $c_r = \delta_{r,1}$ , can be solved for the special case  $A(a) \propto e^a$  for  $a < 0$  by the methods outlined earlier, but much more easily, since Eq. (3.14) is then a linear equation in  $P(\omega; y)$ . Using the form of  $A(a)$  in Eq. (3.11), we obtain

$$\mu(y) = (1-g) \frac{1+g - \sqrt{4(1-y)g + (1-g)^2}}{2g}. \quad (3.22a)$$

The branch cut moves to  $y = 1$  at  $g = g_T = 1$ ; the threshold thus occurs when the mean value of  $a$  is zero. For  $g = 1 - \epsilon$  the scaling form of  $\mu(s)$  is

$$\mu(s) \sim \epsilon \exp[-\epsilon^2 s/4]/s^{3/2} \quad (3.22b)$$

which yields  $\kappa = 0$  and  $\nu = 2$  as in Eq. (2.22). The mean polarization can be obtained as for the mean-field case, giving  $\gamma = 2$ , also in agreement with Eq. (2.22) [and Eq. (3.2)]. Thus the only physical dimension for which we do not have an analytic solution is the case of  $d = 2$ , for which we must resort to numerical studies.

### F. Finite-size scaling and exponent bounds

It is useful to consider the finite-size scaling of various quantities for the analysis of our numerical results in two dimensions. We assume that, below threshold, the scaling of appropriate quantities in a finite system of length  $L$  and width  $\propto \sqrt{L}$  in the transverse directions (corresponding to  $\xi_{\perp} \sim \sqrt{\xi}$ ) is related to that in infinite systems, with scaling functions of  $L/\xi$ . For example, the fraction of sites connected to both the top and the bottom is expected to scale as Eq. (3.1), i.e.,

$$\rho_c(L, F) \sim \frac{1}{L^{\kappa}} \hat{\rho}_c(L/\xi). \quad (3.23a)$$

Right at threshold,  $\xi$  diverges, and there are treelike incipient infinite clusters that span the system, connecting it from top to bottom. The fraction of sites connected to both top and bottom scales as

$$\rho_c(L, F_T) \sim 1/L^{\kappa}. \quad (3.23b)$$

The average number of incipient infinite or spanning clusters, defined as those clusters connected to both top and bottom, is

$$\bar{N}_c(L, 0) \sim L^{\frac{d+1}{2} - \kappa - d_f}, \quad (3.24a)$$

which is independent of  $L$  for  $d < 3$ , if Eq. (3.21) is assumed. Away from threshold,

$$\bar{N}_c(L, F) \sim L^{\frac{d+1}{2} - \kappa - d_f} \hat{N}_c(L/\xi). \quad (3.24b)$$

The probability  $p_c(L, F)$ , that there is at least one connection from top to bottom is also expected to be scale independent at threshold.

It is not obvious that the exponent in the prefactor of a finite-size quantity like those in Eqs. (3.24) must be related to the scaling in infinite systems. For instance, the probability of a finite system of length  $L$  being connected from top to bottom is less than the probability for a region of the same size *inside* an infinite system. This is because no fluid enters from outside into a finite system, unlike for an internal region in an infinite system. Equations (3.23) and (3.24) make the implicit assumption that the corrections to finite-size quantities from such boundary effects are not singular. In Appendix B, we shall argue that this assumption is valid in mean-field theory. In two dimensions, it is supported by the results of our numerical simulations. However, for  $d = 1$ , finite-size quantities scale differently; this is discussed in detail in Appendix B, where it is argued to be a special case.

The characteristic length of the clusters is expected to scale in the same way in finite and infinite systems. The inequality of Chayes *et al.*<sup>24</sup> for finite-size correlation lengths can then be used to obtain a bound for  $\nu$  in all dimensions. This inequality is obtained from the fact that the sample to sample variations in the threshold field  $F_T$  in finite systems must be at least as large as the variations in the mean height of the random barriers; since the transverse directions scale as  $\sqrt{L}$ , these variations in

the mean height of the barriers scale as  $\sim L^{-(d+1)/4}$ , so that

$$\nu \geq \frac{4}{d+1}. \quad (3.25)$$

This inequality is satisfied for  $d > 3$  by the mean-field result, and is saturated for  $d = 1$ .

For  $d < 3$ , all exponents can be expressed in terms of the two unknown quantities,  $\kappa$  and  $\nu$ . It is possible to place a bound on  $\kappa$ : since the infinite clusters at threshold have to be at least linear in extent,  $d_f \geq 1$ ; Eq. (3.21) then implies

$$\kappa \leq \frac{d-1}{2}. \quad (3.26)$$

Equation (3.25) gives a bound on  $\nu$ . For  $d = 2$ , the only physical dimension for which all the exponents are not known, we thus have  $\kappa \leq 1/2$  and  $\nu \geq 4/3$ .

### G. Numerical simulations in two dimensions

We have performed a numerical finite-size scaling study of the two-dimensional lattice model. The external driving force  $F$  only appears in the combination  $h_i - \min_{\alpha} b_{i\alpha} + F$ . As in the mean-field analysis, we start the system initially with  $h_i + F - \min_{\alpha} b_{i\alpha} = a_i$ , where  $a_i$  is chosen independently at each site from a distribution  $A(a)$ . The system is now equilibrated by moving sequentially from one row to the next downhill; any site for which  $\Delta_i$  (defined earlier in the subsection on mean-field theory) is greater than zero pours out an amount  $\Delta_i$  of fluid over the lowest barrier emerging from it. Since the transverse correlation length,  $\xi_{\perp}$ , scales as  $\sqrt{\xi}$ , the width of a finite size system should scale with its length  $L$  as  $\sim \sqrt{L}$ . We have used systems of size  $L \times 8\sqrt{L}$  for  $L$  in the range 128–4096. The distribution  $A(a)$  was taken to be

$$A(a) = \theta(F - a) \exp[a - F]. \quad (3.27)$$

As a function of  $F$  and  $L$ , the mean polarization  $\Pi$ , the fraction of sites  $\rho_c$  connected to the top and bottom of the system, the average number  $\bar{N}_c$  of spanning clusters, and the first, second, and third moments of the cluster masses and (downhill) lengths were calculated.

The expected scaling of the  $k$ th moment of the cluster length can be obtained from Eq. (3.1) by multiplying the right-hand side by  $l^k$  and integrating over all  $l$ . Since  $\xi \sim |f|^{-\nu}$ ,  $\langle l^k \rangle$  should scale as  $|f|^{(\kappa-k)\nu}$  when  $k > \kappa$ , which is valid for all integer  $k > 0$ , by Eq. (3.26). (The zeroth moment is simply the probability for a site to be in a cluster of length  $l$ , summed over all  $l$ , and thus has to be unity.) The  $k$ th moment of the *mass* of a cluster (i.e., the number of sites in it) should similarly scale as  $|f|^{(\kappa-kd_f)\nu}$  for  $k > 0$ . For finite systems, these moments should then have the scaling forms

$$\langle l^k(L, F) \rangle \sim \frac{1}{|f|^{(k-\kappa)\nu}} \hat{l}_k(L/\xi) \quad (3.28a)$$

and

$$\langle s^k(L, F) \rangle \sim \frac{1}{|f|^{(kd_f - \kappa)\nu}} \hat{s}_k(L/\xi). \quad (3.28b)$$

Similar scaling forms should hold for the fraction of sites connected to the top and the bottom of a finite system, as well as for the average number of spanning clusters, and the mean polarization. Since the singular part of the polarization in an infinite system scales as  $|f|^{1-\gamma}$ , we have

$$\Pi_s(L, F) \sim \frac{1}{|f|^{\gamma-1}} \hat{\Pi}_s(L/\xi). \quad (3.29)$$

As discussed in the previous section, from Eq. (3.23a) the fraction of sites connected to the top and the bottom should exhibit the form

$$\rho_c(L, F) \sim |f|^{\kappa\nu} \hat{\rho}_c(L/\xi), \quad (3.30)$$

and the average number of clusters  $\bar{N}_c$  that connect the top to the bottom should have the scaling form in Eq. (3.24b).

Figure 4 shows a logarithmic plot of the first moment of the cluster lengths. The threshold  $F_T$  is treated as a single adjustable parameter to obtain all the numerical plots. A similar plot for the first moment of the cluster mass is shown in Fig. 5. For  $L \gg \xi$ , these plots should be linear, with slopes given by  $\nu(\kappa - 1)$  and  $\nu(\kappa - d_f)$ , respectively, from Eqs. (3.28). For the largest system sizes we have used, this is valid over a fairly wide range of  $f$ ; the slope of the linear region of the graphs can be used to obtain  $\nu(1 - \kappa) \approx 1.25$ , and  $\nu(d_f - \kappa) \approx 1.62$ . Similar plots can be generated for the second and third moments of the cluster lengths and masses, from which we thereby obtain  $\nu(2 - \kappa) \approx 2.95$ ,  $\nu(3 - \kappa) \approx 4.72$ ,  $\nu(2d_f - \kappa) \approx 3.75$ ,

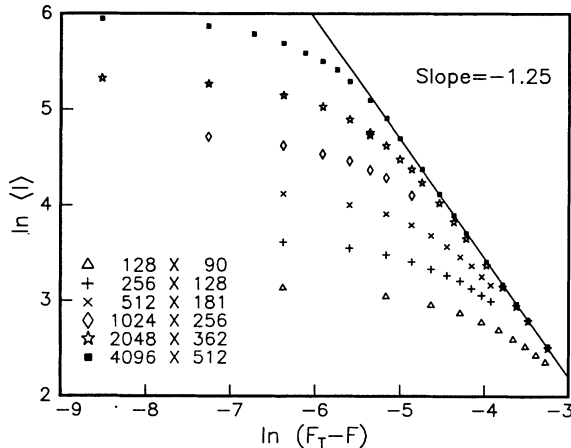


FIG. 4. Plot of the first moment of the cluster lengths,  $\langle l \rangle$ , for different system sizes as a function of distance from the threshold in two dimensions. The threshold was obtained as a fitting parameter for the scaling of the number of connections linking the top to the bottom (shown in Fig. 9), and is the same in all the scaling plots. Both the regions  $L \gg \xi$ , where  $\langle l \rangle$  is independent of  $L$ , and  $L \ll \xi$ , where finite size corrections are present, are seen in the figure. The system sizes,  $L \times 8L^{1/2}$ , are listed with the vertical length first.

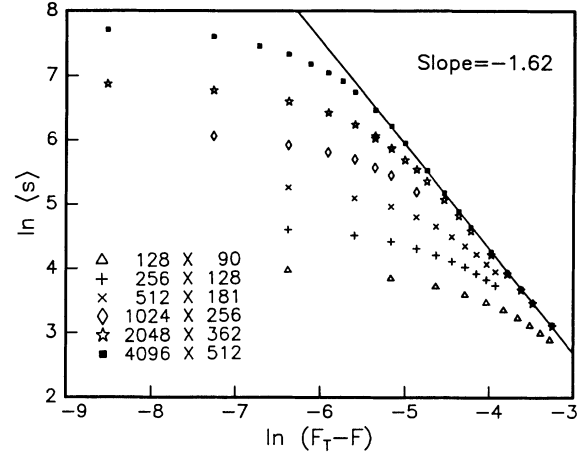


FIG. 5. Plot of the first moment of the cluster size distribution,  $\langle s \rangle$ , for various system sizes in two dimensions.

and  $\nu(3d_f - \kappa) \approx 5.89$ . From the scaling of the cluster lengths, we obtain  $\nu = 1.74 \pm 0.03$  and  $\kappa\nu \approx 0.49 \pm 0.03$ , while from the cluster masses we obtain  $d_f\nu = 2.14 \pm 0.01$ , and  $\kappa\nu \approx 0.52 \pm 0.01$ . (The error bars are estimated from the scatter in the exponents obtained from different moments of the cluster lengths and masses.) Combining these results, we obtain  $d_f + \kappa \approx 1.52 \pm 0.03$ , which is in good agreement with Eq. (3.21). Alternatively, if we use Eq. (3.21), we are left with two independent exponents  $\kappa$  and  $\nu$ , which we estimate as

$$\nu = 1.76 \pm 0.02 \quad (3.31a)$$

and

$$\kappa = 0.29 \pm 0.02 \quad (3.31b)$$

and therefore, from scaling,

$$d_f = 1.21 \pm 0.02. \quad (3.32)$$

Scaling plots can be generated from the data by plotting  $\ln \langle l^k \rangle + (k - 1 - \kappa)\nu \ln |f|$  as a function of  $\ln |f| + (\ln L)/\nu$ , and similarly for  $\ln \langle s^k \rangle + \{(k - 1)d_f - \kappa\}\nu \ln |f|$ . The data for each should all collapse onto a single curve, independent of  $L$ . Figures 6 and 7 show the results for the first and third moments of the cluster lengths. The collapse is poorer for the first moment, possibly due to corrections to scaling that have greater effects on lower moments. Similar plots can be generated from the data for the cluster masses; the quality of collapse also improves here for higher moments.

Figure 8 shows a scaling plot for the fraction of sites connected to the top and the bottom of the system, obtained by using Eq. (3.30) with the values for the exponents found from the scaling of the cluster sizes. A similar plot for the mean number  $\bar{N}_c$  of clusters connecting the top to the bottom obtained from Eqs. (3.24b) and (3.21) is shown in Fig. 9. The probability of the system being connected,  $p_c(L, F)$ , also fits such a scaling form, with  $p_c(L, F_T) \approx 0.32$ .

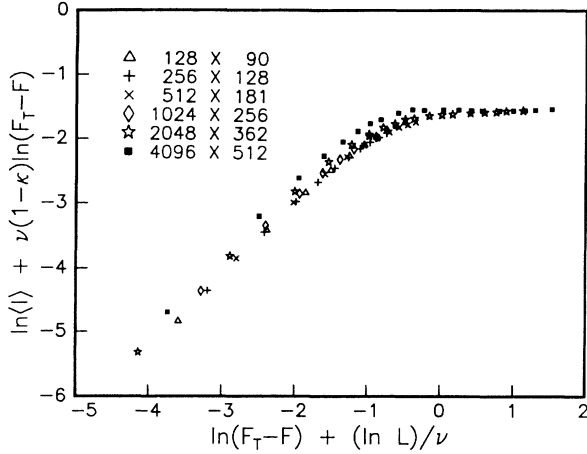


FIG. 6. Scaling plot for the mean cluster length  $\langle l \rangle$  for various system sizes in two dimensions, obtained by using the exponents  $\kappa = 0.29$  and  $\nu = 1.76$ . The collapse of the data for different system sizes onto a single scaling curve is not very good, presumably due to corrections to scaling that affect low moments of the cluster distribution.

From Eq. (3.2), the singular part of the polarization should scale as  $|f|^{1+\kappa\nu-\nu}$ . With our fitted values of  $\kappa$  and  $\nu$  this is  $\sim |f|^{-0.25}$ , i.e.,  $\gamma = 1.25$ . The smallness of the exponent results in the polarization appearing to behave as  $\sim \ln |f|$  over a fairly large range of  $|f|$ , as shown in Fig. 10. The true scaling form for the polarization would be obtained only very close to threshold, for which much larger system sizes are needed to eliminate finite size effects. Figure 11 shows the same data on a logarithmic plot, with the predicted asymptotic slope indicated in the figure. It is not possible to verify whether this slope is correct, although it is consistent with the data. However, the polarizability of the system,  $d\Pi/df$ , is related to the first moment of the cluster lengths, which was seen to scale reasonably well.

We thus see that the numerical results in two dimen-

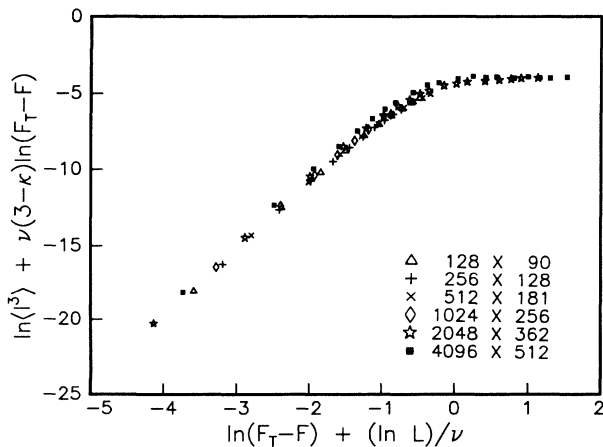


FIG. 7. Scaling plot for the third moment  $\langle l^3 \rangle$  of the cluster length, for various system sizes in two dimensions, with best fit exponents  $\kappa = 0.29$  and  $\nu = 1.76$ , showing a better collapse onto a single curve than in Fig. 6.

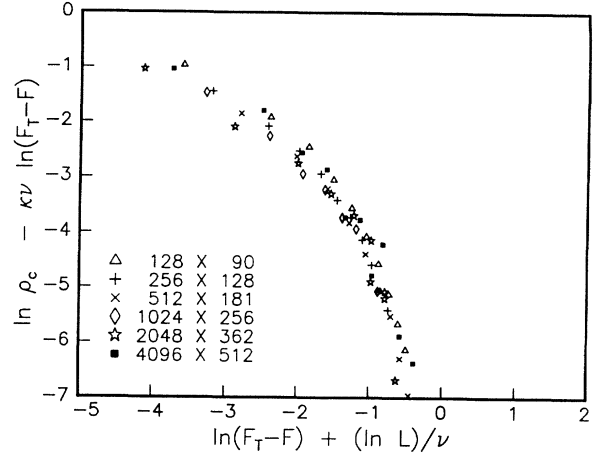


FIG. 8. Scaling plot for the fraction of sites  $\rho_c$  that are connected to the top and the bottom in finite two-dimensional systems of different sizes as a function of the distance from threshold ( $\kappa = 0.29$  and  $\nu = 1.76$ .)

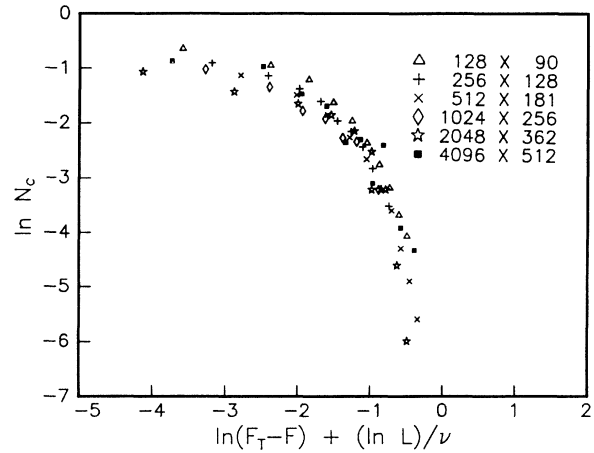


FIG. 9. Scaling plot of the average number  $\bar{N}_c(L, F)$  of connections from top to bottom of a finite two-dimensional system of size  $L \times 8L^{1/2}$ . This should be a function only of  $L/\xi$ . Here, the best fit values from the cluster distribution are used.

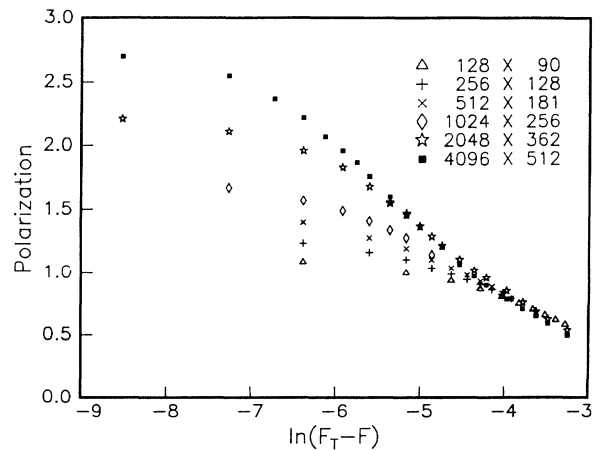


FIG. 10. Polarization density as a function of the distance from the threshold for systems of different sizes in two dimensions. Over a fairly wide range, the polarization density appears to behave as the logarithm of the distance to threshold.

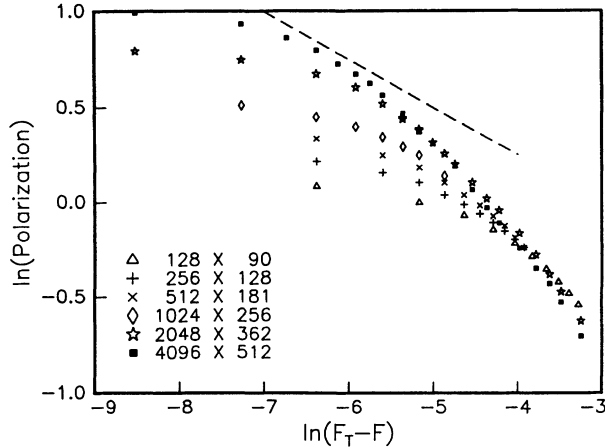


FIG. 11. Polarization density as a function of distance from the threshold on a log-log plot for various sized two-dimensional systems. The straight line shows the predicted slope in the critical regime for large systems; the convergence to this slope for the finite size systems that we have examined is not very satisfactory.

sions seem to be reasonably well fit by the simple scaling laws in terms of two exponents, which satisfy the expected inequalities, Eqs. (3.25) and (3.26).

Our simulations do not yield the correct behavior above threshold. Several changes would be required in order to obtain this correctly. Firstly, it is necessary either to work with very large systems, so that the transient response lasts sufficiently long, or to use appropriate boundary conditions at the top and the bottom of the system. A simpler alternative is to impose periodic boundary conditions connecting the top and the bottom, so that there can be a steady state current circulating through the system. Secondly, one must search for a dynamic steady state, in which at every time step fluid is both input into a site from the row above it and flows out into the row below it. The row by row updating procedure that we have used here is not appropriate above threshold. Finally, fluid can flow out of a site in more than one direction above threshold. In the simulations discussed above, fluid is only allowed to flow out over the lowest barrier from a site, so that even above threshold the clusters are treelike.

#### IV. ABOVE THRESHOLD

In this section, we consider the behavior above threshold, where there are flowing rivers carrying fluid from the top to the bottom of the system. The rivers split and form a network, with a typical downhill separation between splits that can be used to define a correlation length,  $\xi'$ . Infinite clusters appear which contain all the sites that drain into the rivers; these occupy a fraction of the volume which we conjecture to scale as

$$\phi \sim f^\Gamma. \quad (4.1)$$

Since these clusters fill up a finite fraction of the volume

on scales  $> \xi'$ , there is an excess of fluid *density* in them, beyond that which can persist without flowing. The excess fluid will flow through a system of length  $L$  for a time at least of  $O(L)$ . Although this is only a transient, for an infinite system it can be treated as a well-defined steady state (such a state can also be stabilized through periodic boundary conditions at the top and bottom), provided that the fluctuations in current caused by the random initial configuration die out in a finite time (or at least much faster than the “steady state”), so that steady state *can* be reached. We shall return to this issue later. An alternative is to characterize the behavior above threshold in terms of the mean current flowing through the system, which is put in at the top, with “threshold” occurring trivially at zero current. We shall discuss this approach later in this section.

The infinite clusters consist of real rivers, which last for a lifetime that diverges with the system size. These are fed by finite tributary channels which, unlike the real rivers, last only for a short time, and merely augment the amount of fluid in the rivers. One can define the river sites as being those which are monotonically connected to both the top and the bottom of the lattice, while the tributary sites are only monotonically connected to the bottom: to get to the top, one would have to first go down and then up. As the rivers progress downhill, they meander randomly in the transverse directions, and therefore occasionally run into one another, joining to form a single river. If there were no resistance to the flow, once two rivers joined they would not split apart again, so that the flow would occur down a tree with more and more current flowing in the “trunk” as the rivers progressed downhill. However, this cannot be the case. The depth of the rivers has to increase with the flow rate according to Eq. (2.3). Eventually, when at some site  $i$  there is more than one outlet barrier  $\alpha$  for which  $h_i > b_{i\alpha} - F$ , the fluid will spill out through secondary outlets. New rivers are thus formed, which fork off downwards. These rivers can then recombine as before, and, far from the top of the system, there will be an equilibrium between rivers splitting and joining.

Figure 12 shows the flow pattern in the system above threshold. There are three types of sites: (a) *Isolated sites* in finite clusters, where small amounts of additional fluid will just go to the lake at the terminus of the cluster, but will not cause them to overflow. These sites are effectively disconnected from the flow. (b) *Tributary sites*, which drain into the rivers in a finite amount of time, so that there is no steady state flow through them. After the initial equilibration time, all the sites in these tributaries are filled to capacity, so that any more fluid poured in them would flow into the rivers. (c) *Flowing river sites*, which have a nonzero steady state current flowing through them.<sup>25</sup> These sites are analogous to the backbone of the infinite clusters in conventional percolation above threshold.<sup>14,15</sup> Some of these sites are not present in the infinite cluster *at* threshold, but are included in the flowing rivers because of the splitting of the rivers. The density of sites of types (b) and (c) together defines  $\phi \sim f^\Gamma$ , with the tributary sites attached as appendages to the backbone. The density of flowing river sites, i.e.,

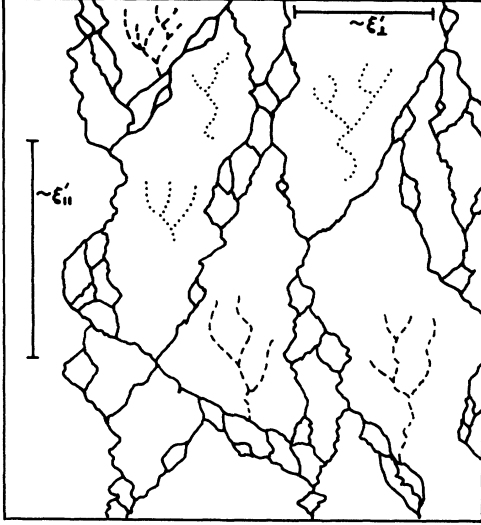


FIG. 12. Schematic of the distribution of rivers above threshold for a two-dimensional system. On the scale of the figure, the lattice is essentially a continuum. Flowing rivers are shown with solid lines, tributaries with dashed lines, and isolated clusters with dotted lines. The number of isolated clusters will in reality be much more, but has been reduced in the figure for clarity. The characteristic correlation lengths are indicated in the figure. The typical distance between splits is much less than  $\xi'$ .

of type (c), defines  $\phi_R$ , which by consistency cannot be greater than  $\phi$ ; we shall later verify that it is in fact much smaller near threshold in all dimensions  $d > 1$ .

We expect that above threshold, due to splits in the rivers, a steady state river distribution will be reached in a finite downhill distance, and  $\xi'$  and  $\xi'_\perp$  will be finite. Since the splits, which cause the finite correlation length above threshold, have no analog below threshold, it is not clear that the correlation lengths on the two sides of the transition should scale the same way; indeed, we will find that they do not.

We assume a scaling form for the fraction of sites connected to both the top and the bottom in a finite system of size  $L$  (i.e., flowing river and tributary sites) similar to Eq. (3.23a), but with *different* exponents:

$$\phi(L, f) \sim \frac{1}{L^{\Gamma/\nu'}} \hat{\phi}(L/\xi'). \quad (4.2)$$

From the scaling *at* threshold, which has to agree with Eq. (3.23b), we obtain

$$\Gamma/\nu' = \kappa. \quad (4.3)$$

On scales much greater than  $\xi'$  the total volume occupied by the infinite clusters will be  $\sim Vf^\Gamma$ , where  $V$  is the volume of the system. All the tributary sites in the infinite clusters are filled to capacity, while the flowing river sites have an excess amount of fluid that causes current to flow. Since the capacity of any site decreases linearly with  $F$ , an increase in  $f$  by  $\delta f$  will reduce the total capacity of the sites in the infinite clusters by  $\sim Vf^\Gamma \delta f$ , thereby increasing the excess fluid in the clusters by the

same amount. All this excess fluid must be present in the flowing river sites, since the tributaries drain into them. Thus the total excess fluid in the flowing river sites for small  $f$  is  $\sim Vf^{1+\Gamma}$ .

### A. Correlation lengths

We now analyze the statistics of the rivers. We shall first consider the nature of the pattern of the flowing river sites, and the appropriate definitions of the correlation lengths, and try to obtain how they scale. We will also obtain the scaling of the average current carried across the system which, unlike the other quantities, depends on the system-dependent local exponent  $\beta_0$ , introduced in Eq. (2.3), that controls the local flow rate. We define the depth of a river at site  $i$  by  $\delta_i = h_i + F - \min_\alpha(b_{i\alpha})$ , in terms of the steady state value of  $h_i$ . The total amount of fluid that causes the flow is  $\delta_{\text{tot}} = \sum_{\text{river sites}} \delta_i$ . This should equal the excess fluid from all the river and dry river sites, which scales as  $Vf^{\Gamma+1}$ . The typical depth of a river is thus  $\bar{\delta} = \delta_{\text{tot}}/(V\phi_R)$ , where  $\phi_R$  is the density of flowing river sites. If the rivers form a network with a typical transverse distance  $w$  between rivers, then  $\phi_R \sim w^{(1-d)}$  and

$$\bar{\delta} \sim f^{\Gamma+1}/\phi_R \sim f^{\Gamma+1}w^{(d-1)}. \quad (4.4)$$

The typical downhill distance between forks of rivers is determined by the probability that  $\delta_i > \min_{\beta \neq \alpha}(b_{i\beta} - \min_\alpha b_{i\alpha})$ , i.e., that the depth of fluid exceeds the height of the second lowest outlet barrier. If the distribution of barrier heights  $B(b)$  is smooth around  $\min_\alpha b_{i\alpha}$ , then the probability of this is of the order of  $\delta_i$ , so that the typical downstream distance between forks is  $l_F \sim 1/\bar{\delta}$ .<sup>26</sup> Naively, one would expect  $w$  to be the transverse correlation length  $\xi'_\perp$ , and  $l_F$  to be  $\xi'$ . However, the first is found to be an appropriate definition only for  $d < 3$ , while the second is appropriate for  $d > 3$ . We first analyze the case of  $d < 3$ .

#### 1. $d < 3$

Above threshold in  $d < 3$ , the effects of splits of the rivers is somewhat subtle. The typical distance between these forks is of order  $l_F \sim 1/\bar{\delta}$  as above, but with probability close to unity, the two branches that emerge from a split recombine in a short distance downstream. It is simplest to understand this problem by viewing the rivers as particles performing independent random walks in a  $(d-1)$ -dimensional space, with the downhill direction as time. The two branches emerging from a split are equivalent to random walks that start from the same point. For  $d-1 < 2$ , the probability that these two random walks do *not* combine before a “time”  $l$  downstream is

$$p_N \sim 1/l^{\frac{3-d}{2}} \quad (4.5)$$

(with a logarithmic decay for  $d = 3$ ). If, after a river forks, the two branches recombine rapidly, then under coarse graining the split will only appear as an increase

in the effective thickness of the river rather than a true branching of the river. One thus needs to consider only those splits after which both branches survive for sufficiently long. The consistency condition to be used to determine this is that the two branches should last long enough to spawn other branches that also last comparably long. Only these branches will appreciably lower the mean depth of the rivers, which is the quantity determining the splitting probability. Using Eq. (4.5), the probability per unit length of creating a branch of length  $l$  is  $\sim l^{(d-3)/2}/l_F$ . Since we want the probability of spawning such a “long” branch from a section of length  $\sim l$  to be  $O(1)$ , the consistency condition is

$$l \sim l^{3-d/2} l_F. \quad (4.6a)$$

The downhill correlation length  $\xi'$  is the typical distance between such “true” splits:

$$\xi' \sim l_F^{2/(d-1)} \sim (1/\bar{\delta})^{2/(d-1)} \quad (4.6b)$$

which, for  $d < 3$ , is much greater than  $l_F$ , the naive correlation length.

In order for an equilibrium to be established between splitting and recombination of such long-lasting rivers, the branches must combine with other rivers (i.e., different from the one they branched off from) a significant fraction of the time. These recombinations raise the depth of the rivers, making them more susceptible to splitting. We define  $\xi'_\perp$  as being the typical transverse distance between recombinations, which is the distance out to which the current is strongly correlated. For  $d < 3$ , this is equal to the mean separation between the rivers,  $w$ , since two rivers cannot cross through each other without “colliding,” and thereby joining together.<sup>27</sup> (For  $d \geq 3$ , the rivers can intertwine around each other, and move over distances much larger than  $w$ , although this is unlikely in three dimensions.) Since the transverse motion is a random walk, the downhill distance between recombinations is  $\sim (\xi'_\perp)^2$ . This has to be equal to  $\xi'$  in equilibrium. Replacing  $\xi'_\perp$  by  $\xi'^{1/2}$  in Eq. (4.4), and using Eq. (4.6b), we obtain

$$(d-1)\nu' = \Gamma + 1. \quad (4.7)$$

This can be combined with Eq. (4.3) to yield  $\Gamma$  and  $\nu'$  in terms of the corresponding exponents below threshold:

$$\nu' = 1/(d-1-\kappa) \quad (4.8a)$$

and

$$\Gamma = \kappa/(d-1-\kappa). \quad (4.8b)$$

Since  $\phi_R = w^{1-d}$ , and  $w \sim \xi'_\perp \sim (\xi')^{1/2}$ , we have

$$\phi_R \sim f^{(1+\Gamma)/2}. \quad (4.9)$$

Note that all the exponents above threshold depend on *one* of the exponents ( $\kappa$ ) below threshold. The other exponent,  $\nu$ , does not affect the equilibrium behavior above threshold, although it should affect the *approach* to equi-

librium. A schematic illustration of the river pattern with its multiple length scales is shown for  $d = 2$  in Fig. 12.

## 2. $d \geq 3$

We now turn to the case of  $d > 3$ . The behavior above threshold can be analyzed straightforwardly. Since in  $d > 3$  a positive fraction of the rivers that split will not rejoin, the downstream distance  $\xi'$  between “true” splits, from which the branches emerging do not rejoin, scales in the same way as  $l_F$ . These river branches will recombine with other rivers, which have density  $\phi_R$ . These can be considered to be approximately randomly distributed, since the different rivers can intertwine and pass by each other in high dimensions. The recombination probability is thus  $\sim \phi_R$ . The condition for the splitting and recombination processes to balance is now

$$\xi' \sim l_F \sim 1/\phi_R, \quad (4.10)$$

implying that

$$\phi_R \sim f^{\nu'}, \quad (4.11)$$

and the typical distance between rivers is

$$w \sim f^{-\nu'/(d-1)}. \quad (4.12)$$

As mentioned previously, this is *not* the transverse correlation length. The current is strongly correlated over transverse distances  $\xi'_\perp \sim \sqrt{\xi'}$ . (This is also the case for  $d < 3$ , however,  $\xi'_\perp$  is much greater than  $w$  for  $d > 3$ .) Combining Eqs. (4.10) and (4.11) with (4.4), we have

$$2\nu' = 1 + \Gamma \quad \text{for } d > 3. \quad (4.13)$$

At the upper critical dimension,  $d = 3$ , Eqs. (4.7) and (4.13) are equivalent, and, from Eq. (4.12),  $w \sim \xi'_\perp$ . There will, as below threshold, probably be logarithmic corrections to various quantities in three dimensions.

## 3. General $d$

Before combining the various results to obtain the exponents above threshold, we consider an alternate argument which yields the scaling of  $\bar{\delta}$  in any dimension. This method does not require an analysis of the correlations between the positions of the various rivers; however, it also does not involve the parallel correlation length  $\xi'$ , and therefore does not bring out the difference between  $l_F$  and  $\xi'$  in low dimensionality. It is useful to work in the picture in which the downhill direction corresponds to “time.” We first consider a slightly different system, where the rivers do not split into branches, nor do they join together when two of them meet. This is equivalent to independent particles performing random walks which can pass through each other. Figure 13(a) shows

a typical region of the system. With short range correlations in the initial conditions, sufficiently far downhill, the positions of the different particles are random and uncorrelated. In any row of the lattice, the probability of a specific river intersecting with some other one is then  $\sim \phi_R$ . Now we perform the following transformation: in any row (each row corresponds to a particular time in the particle picture) for each of the sites where two particles are present, we move one to some other randomly chosen site which has only one particle present. Subsequently, we time-evolve this modified configuration as before. Since the future course of a particle (for instance, the duration until its next intersection) depends on the distances to its neighbors, the subsequent behavior of the system will be changed by the transformation. However, for any particle in the original configuration the distribution of distances to its neighbors (apart from any on the same site) is independent of the number of other particles present at its site. Thus in the limit of infinite system size, the transformation of the configuration of particles in one row will not affect the future behavior of the system. Figure 13(b) shows the transformed system; now when two particles meet at the same site, they join into a single one, while there are also random bifurcations of particles into two. The number of bifurcations in

any row is exactly equal to the number of combinations. From our original perspective of flowing rivers, this is just the system we wish to analyze.<sup>28</sup> Since each intersection of paths in the version with intersecting random walks now corresponds to a bifurcation of rivers, equating the probabilities of the two yields

$$\bar{\delta} \sim \phi_R. \quad (4.14)$$

Using the fact that the excess fluid density in the system,  $\sim f^{\Gamma+1}$ , has to be equal to  $\phi_R \bar{\delta}$ , we obtain

$$\phi_R \sim \bar{\delta} \sim f^{(1+\Gamma)/2}. \quad (4.15)$$

This equation is valid in all dimensions, and agrees with our previous results from Eq. (4.9) for  $d < 3$ , and Eqs. (4.11) and (4.13) for  $d > 3$ .

Using the mean-field exponent  $\kappa = 2/3$  from Eqs. (3.16), (3.17), and (3.19), and substituting in Eqs. (4.8), we obtain the *mean-field exponents* above threshold

$$\Gamma = \frac{1}{2}, \quad \nu' = \frac{3}{4}, \quad \text{and} \quad \nu'_\perp = \frac{3}{8}. \quad (4.16)$$

For  $d < 3$ , using Eq. (3.26) with Eqs. (4.3) and (4.7) yields  $\nu' < 2/(d-1)$ , from which  $\Gamma < 1$ . The consistency condition,  $(1 + \Gamma)/2 \geq \Gamma$ , which is required for  $\phi_R$  to be  $\leq \phi$ , is thus satisfied in all dimensions.

Although the inequalities  $\nu' < 2/(d-1)$  and  $\nu > 4/(d+1)$  from finite size scaling do not rule out the possibility of the correlation length exponents being the same, we have seen that they are unequal in mean field, and there is no reason to expect them to be otherwise in general dimensionality. In fact, the mean-field exponent  $\nu'$  is *less* than  $4/(d+1)$  for  $d < 13/3$ . This is not inconsistent because, for  $F > F_T$ , the behavior in any region is affected by other regions that are much further than  $\xi'$  away; this is unlike the case for  $F < F_T$ , where regions of size  $\sim \xi$  are essentially isolated from one another, and thus the finite size scaling and bulk correlation lengths should be similar.<sup>29,30</sup>

In two dimensions, our numerical results, Eqs. (3.31), can be combined with Eqs. (4.8) to give

$$\nu' = 1.41 \pm 0.04 \quad \text{and} \quad \Gamma = 0.41 \pm 0.04. \quad (4.17)$$

It is now possible to verify the hyperscaling assumption for  $d < 3$ , that led to Eq. (3.21). Using Eqs. (4.7) and (4.15), we see that the number of rivers in a correlation volume is independent of  $f$ . Thus the number of rivers in a finite size system will only be a function of  $L/\xi'$ . This implies that *at* threshold, where  $\xi'$  diverges, the number of rivers in a system of length  $L$  and transverse dimensions  $\sim \sqrt{L}$  should be independent of  $L$ . However, as discussed in Eq. (4.3), the connections from top to bottom of a finite system at threshold, that are viewed as rivers if

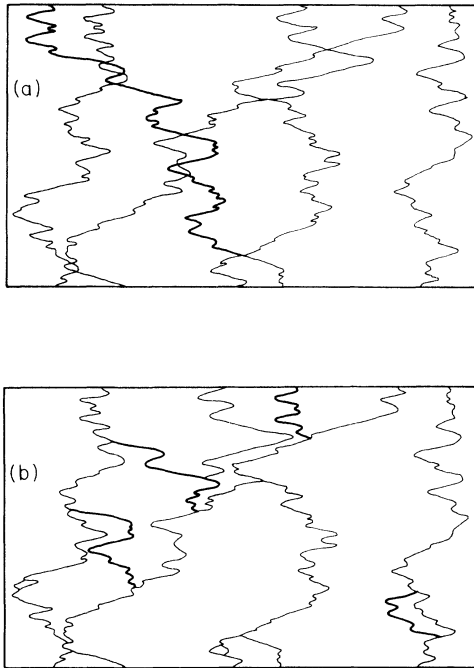


FIG. 13. (a) Typical pattern generated by a set of directed random walks, that move steadily downward with random transverse meanderings. The walks are allowed to intersect. (b) The same pattern, with one of the walks emerging from each intersection being moved laterally to form a split of another walk. The result is similar to the river patterns that are generated in our model. For comparison, one of the sections that is moved laterally is highlighted in both figures.

threshold is approached from above, can be treated as incipient infinite clusters if one approaches threshold from below. From Eq. (3.24a),  $\bar{N}_c(L, 0)$  is seen to be independent of  $L$  only if  $\kappa + d_f = (d + 1)/2$ , i.e., Eq. (3.21).

### B. Scaling of the current

We now find the mean current transported across the system. The average current flowing in the rivers is the average of  $\delta^{\beta_0}$ . It is possible to see that, in a statistical sense (i.e., averaging over different realizations of the randomness) the entire distribution of  $\delta$ 's scales uniformly with  $\bar{J}$ , so that the average current flowing in a river is of the order of  $\bar{\delta}^{\beta_0}$ . For any specific realization of randomness, changing  $\bar{J}$  does not result in a uniform rescaling of all the  $\delta$ 's. At any split in a river, the depths in the two channels that emerge,  $\delta_1$  and  $\delta_2$ , are related by  $\delta_1 - \delta_2 = b_{i2} - b_{i1}$ . This is an inhomogeneous relation, which prevents uniform rescaling of the  $\delta$ 's. However, for small  $\delta$ 's, with a smooth distribution of barrier heights,  $\delta_2$  is uniformly distributed over  $[0, \delta_1]$ , so that  $\langle \delta_1 \rangle = 2\langle \delta_2 \rangle$ . Thus homogeneity is recovered statistically. If the behavior were to be dominated by anomalously large  $\delta$ 's, it would not be possible to assume that the distribution of barrier heights is uniform, since  $b_{i2} - b_{i1}$  could be large. In such a case, the argument above would not be valid. Although we cannot disprove this possibility in general, in Appendix C it is shown that, at least in mean field, this does not happen, and we expect that, in general, small  $\delta$ 's will dominate.

Assuming this domination by small  $\delta$ 's, the mean current density is  $\bar{J} \sim \bar{\delta}^{\beta_0} \phi_R$ . If we define the exponent  $\beta$  through  $\bar{J} \sim f^\beta$ , using Eq. (4.15) we obtain

$$\beta = \left[ \frac{1 + \Gamma}{2} \right] (1 + \beta_0). \quad (4.18)$$

This relation is valid both for  $d > 3$  and  $d < 3$ . (Note that  $\beta$  can be less than or greater than  $\beta_0$ , depending on the magnitude of  $\beta_0$  and  $\Gamma$ .) Equation (4.18) is not valid for the special case of  $d = 1$ . This is because there is a single river extending over the entire system in  $d = 1$ , without any splits. Thus  $\phi_R$  does not scale with  $f$ . Also, the entire system participates in the flow, so that  $\Gamma = 0$ . Comparing with Eq. (4.4), we have  $\bar{\delta} \sim f$ , so that  $\beta = \beta_0$  in one dimension, as could have been anticipated since the current over every barrier is the same.

### C. Current driven system

As mentioned earlier, it is possible to characterize the behavior of the system above threshold in terms of the mean current,  $\bar{J}$ , that flows through the system, instead of  $f$ . This has the advantage of not being sensitive to boundary conditions. There is no equivalent of the exponent  $\Gamma$  in this case, since all properties of the flow can be expressed in terms of the flowing river sites. Furthermore, since  $f$  is no longer a meaningful concept, the exponent  $\nu'$  no longer exists, but instead  $\xi' = \xi'(\bar{J})$ . From

Eqs. (4.14) and (4.18), we have  $\phi_R = \bar{\delta}$ , and  $\bar{J} \sim (\bar{\delta})^{1+\beta_0}$ , so that

$$\phi_R \sim \bar{J}^{1/(1+\beta_0)}. \quad (4.19)$$

From Eq. (4.6b),

$$\xi' \sim 1/\bar{J}^{2/[(d-1)(1+\beta_0)]} \quad (4.20a)$$

for  $d < 3$ . For  $d > 3$ , where  $\xi' \sim 1/\bar{\delta}$ ,

$$\xi' \sim 1/\bar{J}^{1/(1+\beta_0)}. \quad (4.20b)$$

As before,  $\xi'_\perp \sim \sqrt{\xi'}$ . In Appendix C, we construct a mean-field approximation of the system above threshold, specified in terms of currents, and analyze it for the special case of  $\beta_0 = 1$ . We verify Eqs. (4.19) and (4.20b) in this case, finding  $\phi_R \sim 1/\xi' \sim \sqrt{\bar{J}}$ . Note that the current driven formulation is more closely related to finite temperature behavior, which we consider in the next section.

### D. Convergence to steady state

So far we have not demonstrated the uniqueness of the solution we have obtained. If we *specify* all the current inputs at the top of the system, then there must be a *unique* solution, provided that the local  $J(h)$  in Eq. (2.3) is monotonic. This follows from a convexity argument: first note that, because current is conserved locally, the difference between two different solutions can only be a set of current loops that are either closed, or are open at the lower boundary of the system. (See Fig. 14.) In either case, the topmost site of the loop is located inside the system. If we consider the loop with current  $\delta J$  flowing in it shown in the figure, the difference between the two solutions  $a$  and  $b$  is given by  $J_{i1}(a) - J_{i1}(b) = \delta J$ , and  $J_{i2}(a) - J_{i2}(b) = -\delta J$ . Since the current flowing through a link is a monotonic function of the depth of fluid in the site at its upper end, the first of these two implies that

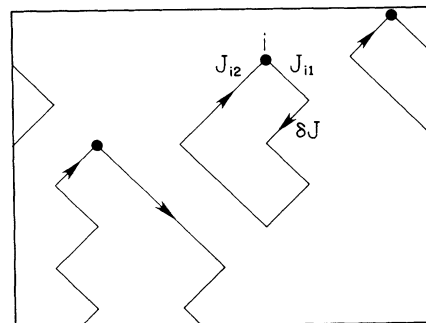


FIG. 14. Schematic of the proof of the uniqueness of the pattern of currents, given the inputs at the top. The difference between two putative distributions of currents for a single system, which both have the same input currents at the top (and periodic boundary conditions on the sides), is shown. The solid circles denote the topmost sites for each of the current loops, which are shown in the text to have contradictory conditions imposed on them.

$h_i(a) > h_i(b)$ , while the second one implies  $h_i(a) < h_i(b)$ . It is thus impossible to assign a depth to the fluid in the topmost site of a loop that is consistent with the current flowing out of it in both directions for both solutions. Therefore the steady state is unique.

The current input at each site at the top can be varied independently, and the resulting solution has to be a function of all of these. As one proceeds down into the system, the effects of these variations will diffuse away.<sup>31</sup> For example, if we put current into only a small fraction of the sites at the top, the channels that emerge from them will split in a downhill distance less than  $\xi'(\bar{J})$ , since the current flowing in these few channels is much larger than what one would normally have at a current density  $\bar{J}$ . Naively, this would seem to imply that in a few correlation lengths downhill, there will be convergence to the steady state bulk statistical behavior. However, the current is conserved locally, and can only move from one region to another by “diffusion.” If we coarse grain the system on scales much larger than the transverse correlation length, the evolution of the current distribution across the system obeys the approximate equation

$$\partial_z J(\mathbf{x}, z) = \nabla_{\mathbf{x}}^2 J(\mathbf{x}, z) + \nabla_{\mathbf{x}} \cdot \boldsymbol{\eta}(\mathbf{x}, z), \quad (4.21)$$

where  $z$  is the downhill coordinate and  $\mathbf{x}$  is the transverse coordinates. Since we have coarse grained on scales much larger than  $\xi_{\perp}$ ,  $J(\mathbf{x}, z)$  can be treated as a continuous variable. The second term in Eq. (4.21) involves a random  $\boldsymbol{\eta}(\mathbf{x}, z)$ , that arises from the local variations of the barrier heights, and has short range correlations:  $\langle \boldsymbol{\eta}(\mathbf{q}, z) \boldsymbol{\eta}(\mathbf{q}', z') \rangle = \langle \eta^2 \rangle \delta(\mathbf{q} + \mathbf{q}') \delta(z - z')$  on Fourier transforming to  $\boldsymbol{\eta}(\mathbf{q}, z)$  and  $J(\mathbf{q}, z)$ . We then have

$$J(\mathbf{q}, z) = \exp[-q^2 z] \left\{ J(\mathbf{q}, 0) + \int_0^z dz_1 \mathbf{q} \cdot \boldsymbol{\eta}(\mathbf{q}, z_1) \exp[q^2 z_1] \right\}. \quad (4.22)$$

The correlations in  $J(\mathbf{q}, z)$  can be obtained by averaging over  $\boldsymbol{\eta}$ , yielding

$$\langle J(\mathbf{q}, z) J(\mathbf{q}', z') \rangle = \langle \eta^2 \rangle \delta(\mathbf{q} + \mathbf{q}') \exp[-q^2 |z - z'|] \quad (4.23a)$$

for large  $z$  and  $z'$ , and hence

$$\langle J(\mathbf{q}, z) J(\mathbf{q}', 0) \rangle = \langle J(\mathbf{q}, 0) J(\mathbf{q}', 0) \rangle \exp[-q^2 z]. \quad (4.23b)$$

Equations (4.23) give the correlations of the current variations inside the system, as well as the response to perturbations in the inputs at the top of the system. Fourier transforming Eq. (4.23a), we obtain

$$\langle J(\mathbf{x}, z) J(\mathbf{x}', z') \rangle \sim \frac{\exp[-(\mathbf{x} - \mathbf{x}')^2 / |z - z'|]}{|z - z'|^{d/2}}. \quad (4.24)$$

For large  $z - z'$ , this yields an asymptotic power-law decay of the form  $\sim |z - z'|^{-d/2}$  in the downhill correlations of  $J$ . Hence the effects of inputs at the top will decay only

as a power of the downhill distance.

In the mean-field analysis in Appendix C, the fact that current can only diffuse from one region to a neighboring one is ignored (the concept of neighboring regions itself being lost). This eliminates the constraint that gives rise (in any dimension) to power laws in the current correlations, and the effects of variations in the inputs at the top boundary are instead found to decay away exponentially in a distance  $\sim \xi'$  into the system.

## V. MODIFICATIONS AND RELATED MODELS

In this section, we discuss the effects of various modifications that are natural to consider for the model we have analyzed so far. We also establish connections with earlier work on related models.

### A. Boundary conditions and equilibration

So far we have largely ignored the question of boundary conditions on the system. This would seem to be difficult to justify, since above threshold the current flowing through the system is determined by the current input at the top boundary. (Since the current flows downhill on the average, the boundary conditions chosen in the transverse directions are relatively unimportant, and may be taken to be periodic for convenience; this is not true at the top and the bottom.) Although the solution that we have obtained can certainly be considered as at least a transient one whose lifetime diverges with the system size and is therefore well defined, for physical systems the true steady state solution at infinite time is likely to be more important. As we have mentioned, it is in fact often possible to neglect boundary conditions as we have done and still obtain the long time bulk behavior.

If in any specific system the analogue of the fluid density  $\bar{h}$  is fixed externally, independent of the driving force  $F$ , then the choice we have made of constant  $\bar{h}$  is clearly appropriate. The driving force  $F$  can be created by imposing a potential difference  $V$  between the top and the bottom. Typically, some of this potential drop,  $V_s$ , will occur at the boundaries, in order to drive a current into (and out of) the system across the boundaries. Thus the actual potential difference in the interior of the system between the top and the bottom will be  $V - V_s$ . For a fixed current,  $\bar{J}$ , the boundary voltage  $V_s$  is *independent* of the length  $L$  of the system, whereas  $V - V_s$  varies linearly with  $L$ . Therefore, for large systems, one can neglect  $V_s$ , and obtain  $\bar{J}$  as a function of  $V$  without reference to the exact details of the boundary effects.<sup>32</sup>

In other systems, the force is effectively imposed by requiring a density difference  $\Delta \bar{h}$  between the top and the bottom, with a mean density  $\bar{h}$  determined externally. (For example, in the mixed state of type-II superconductors,  $\Delta \bar{h}$  is produced by an electric current, and  $\bar{h}$  is fixed by an external magnetic field.) In the absence of randomness, the difference in the density between the top and the bottom will result in a linear change in  $\bar{h}$  across the system. If  $\Delta \bar{h} \ll \bar{h}$ , we may approximate the system as having a uniform density throughout, with the gradient

produced by  $\Delta\bar{h}$  being roughly equivalent to a uniform force across the system. This profile will, of course, be modified by randomness, which will produce variations in the force from point to point; we have modeled these by the local slope of our irregular surface. Unfortunately, in this case, which is limited to the regime  $\Delta\bar{h} \ll \bar{h}$ , it is not possible to take the thermodynamic limit. This is, however, the actual situation in the mixed state of type-II superconductors.

In the case of a real fluid flowing on an inclined surface, it is perhaps more natural above threshold to work with fixed total current as discussed in the previous section, treating  $\bar{J}$  as being externally determined, and expressing other physical quantities as functions of  $\bar{J}$ . The mean depth of fluid  $\bar{h}$  automatically adjusts itself to produce this current; in particular, by fixing  $J = 0^+$ ,  $\bar{h}$  adjusts itself so that  $F = F_T(\bar{h})$ , and the system is at a “self-organized” critical point.<sup>33</sup> [Note that  $F_T(\bar{h})$  from this procedure will *not* be the same as if an initial  $\bar{h}$  is given and allowed to equilibrate in an infinite system, as, in the current driven case, there are no finite clusters.]

Both below and above threshold, there are time scales that diverge at threshold, and can appear to round out the transition. (These are in addition to finite size effects, that occur when  $\xi$  becomes comparable with the length of the system.) As threshold is approached from below, any increase in the force  $F$  results in larger and larger amounts of fluid being displaced before the system returns to equilibrium. With any *finite* rate of increase of  $F$ , this eventually leads to some sites temporarily having a large amount of fluid in them, so that fluid flows out from them in more than one direction, thereby destroying the tree structure even before threshold is reached. Above threshold, there is an initial equilibration time during which the excess fluid in the tributaries drains into the rivers; this time diverges at threshold along with the length of the typical tributary. For any finite system, sufficiently close to threshold, the “steady state” solution that we have analyzed, which is actually a transient with a lifetime diverging with the system size, will never be achieved.

### B. Thermal fluctuations

The most important effect that will modify the behavior discussed so far is that of thermal fluctuations. Our analysis has implicitly been at zero temperature, in the sense that when the depth of fluid in a site is less than the height of one of its outlet barriers, *no* current flows through that outlet. By contrast, at any finite temperature, there will be thermally activated movement of fluid over the barriers. Such processes will result in transport currents at any nonzero  $F$ . A natural form to take for small thermal creep current over a barrier is

$$J_{i\alpha} \sim T^{\beta_0} \Phi\left([F + h_i - b_{i\alpha}]/T\right) \quad (5.1a)$$

with

$$\begin{aligned} \Phi(x) &\sim x^{\beta_0} \quad \text{for } x \gg 1 \\ &\sim \exp[x] \quad \text{for } -x \gg 1 \end{aligned} \quad (5.1b)$$

corresponding to nonactivated flow in the first limit and activated flow in the second. The prefactor in Eq. (5.1a) is chosen to make the effect of thermal fluctuations equivalent to raising the depth of the fluid occasionally to be above the barrier. (Depending on the nature of the thermal fluctuations, the exponent of this prefactor could be different, in which case the specifics of the subsequent results would be changed.)

There are several different regimes, in which the effect of thermal fluctuations are rather different. At zero temperature, it is possible to treat each barrier as permitting flow in one direction (downhill) only. This is because the tilt disfavors uphill flow, so that on long length scales fluid only moves downwards. At finite temperature, however, when the tilt  $F$  is much less than the temperature  $T$ , it is clear that both forward and backward flow are almost equally important. The *total* current flowing across a barrier is then linear in  $F$ , with no threshold. In the first regime, when  $F \ll T$ , but  $T$  is still very small, the system is equivalent to a network of linear resistors with a wide distribution of resistances, whose behavior is known.<sup>34</sup> (At high temperatures, the transport becomes uniform in space and trivial.)

In the second regime,  $T \ll F$ , but the system is still below threshold. When  $T \ll F$ , the transport over a barrier is still effectively unidirectional, as in our model. If  $F$  is much less than the zero-temperature threshold field, there is a nonzero “thermal creep” current. Associated with this, there will be a thermal correlation length that diverges as  $T \rightarrow 0$ . The behavior is, however, rather complicated. Since small thermally activated currents will flow over all the barriers, the fluid depth in any site in the system will eventually reach a steady state value which depends on the thermal currents entering the site; these are in turn determined by the thermal currents flowing much further uphill. Thus to find the equilibrium levels is already nontrivial. Once these levels have been established, the lowest-outlet-barrier tree can be analyzed in a manner similar to that done at zero temperature, and flow will be primarily down this tree, with the thermal current draining out of the tree small unless two outlet barriers at a site are within  $T$  of each other, in which case the current will split as in the zero-temperature case just above threshold. At low temperatures, this will only happen rarely, giving rise to a network of rivers which carry most of the current, with characteristic scales  $\xi_{\parallel}(T)$  and  $\xi_{\perp}(T)$  which diverge at low temperatures and low current density. We will not analyze the behavior in detail here, but only note that at low  $T$ , there will be extremely slow transients as almost isolated lakes fill up by small thermal currents gradually lowering the fluid level in the rest of the system.

Another interesting regime is that near the zero-temperature threshold. One might expect that, at low temperatures, the only effect of thermal fluctuations in this regime would be to round out the transition at  $F_T$ , which is sharp for  $T = 0$ . However, just as in the previous regime, this is not the case: the entire spatial distribution of fluid is altered from its zero-temperature form. At  $T = 0$ , in the critical regime, most of the system does not participate in the fluid flow. Fluid stays trapped in iso-

lated regions; as  $F$  is increased, these isolated regions successively link up to the rivers, producing additional singularities and the nontrivial exponent  $\Gamma$ . At *any* nonzero temperature, however, fluid leaks out of (and into) these previously isolated regions, linking them to the rivers and lowering the level in the rivers as discussed above. This means that the threshold  $F_T^+ \equiv F_T(0^+)$  in the limit of  $T \rightarrow 0$ , which is sharp, is strictly *greater* than the threshold at zero temperature. In addition, the dependence on  $F$  of the mean level in the rivers that dominate the flow for  $F \gtrsim F_T^+$  will be different from the dependence at zero temperature due to the rise in level in the rest of the system; this will modify the critical exponents that can in principle be observed near  $F_T^+$  in the limit of low  $T$ . As discussed above, continuity with  $T = 0$  is maintained through the time scale it takes for the steady state solution to be established: for small  $T$ , the system will behave like the zero-temperature solution for a very long time.

In addition to the qualitative changes discussed above, thermal fluctuations also produce a more conventional rounding out of the transition (at  $F_T^+$ ). Close to the transition, a substantial fraction of the current is thermally activated; although an individual thermally activated channel carries very little current, this is balanced by the small density of the rivers,  $\phi_R$ . The *density* of activated current is proportional to the rate at which it is returned to the flowing rivers, which must in equilibrium be equal to the mean thermally activated current emerging from the flowing rivers. If  $\delta b_i$  is the difference in height between the second lowest and lowest barriers at a flowing river site  $i$ , the activated current emerging from the site is  $\sim T^{\beta_0} \exp[-(\delta b_i - \delta_i)/T]$  from Eq. (5.1). For small  $T$ , this is dominated by small  $\delta b$ , and thus the distribution of  $\delta b_i$  can be taken to be uniform. Integrating over  $\delta b_i$ , we obtain that the mean activated current emerging from a flowing river site is  $\sim T^{1+\beta_0}$ . When this is of the order of  $\bar{J}$ , the transition will be rounded; however the result is sensitive to the form of the creep assumed in Eq. (5.1). We leave more detailed analysis of thermal fluctuation effects for future investigation.

### C. Continuum systems

The model that we have considered so far has been a lattice model, whereas real systems for which it might be directly applicable are mostly continuum systems. In continuum systems, there is a variable width  $w_R$  associated with each river connecting two lakes, in contrast to the lattice model where the link between two lattice sites does not have a variable width. The first effect of this is to produce an extra factor of  $w_R^{d-1}$  in the current flowing in a channel. When the river is confined close to a local minimum of the (smooth) random potential produced by the irregularities of the surface, the variation of the potential around the minimum will be generically quadratic. This is shown in Appendix A to lead to an increase in  $\beta_0$  from its one-dimensional value by an amount  $(d-1)/2$ . The second result of continuum effects is to modify the branching and recombination rates of rivers:

it is possible for two halves of a river of finite width to fall into different local minima of the potential, and diverge in different directions, while the probability of two rivers joining also depends on their widths. In a consistent treatment of the continuum nature of the system, it would be necessary to include the effects of correlations in the surface potential, which is smooth on sufficiently short scales. It is not clear at this point what the overall effect of these modifications would be.

As shown in Appendix A, for *fluid* flow the appropriate value of  $\beta_0$  in one dimension is  $3\frac{1}{2}$  (which we have argued above is generalized to  $3 + d/2$  in  $d$  dimensions). This is because the viscous force depends on velocity *gradients* in the direction perpendicular to the surface. On the other hand, in many systems the drag force is merely proportional to the velocity, especially in cases (as in flux lattices) where there is no equivalent of the direction perpendicular to the surface. This could change  $\beta_0$  to  $1 + d/2$ , or some other value. The exponents involving the current will depend on some of the local details, as is the case for conventional continuum percolation.<sup>22</sup>

### D. Relationship to other work

Several models that bear some qualitative resemblance to the one we have considered here have been studied previously. Below threshold, our model is in a general class of directed percolation models.<sup>17</sup> In standard percolation,<sup>14</sup> one considers a lattice in which each site may be connected to its nearest neighbors through bonds. The probability for the existence of a bond linking two sites is independent of the probability for any other pair of sites. In directed percolation,<sup>17</sup> the bonds are *directional* and the bonds from a site can only go to a restricted set of its nearest neighbors, that are biased in a particular direction. For instance, with a hypercubic lattice, the allowed bonds can be restricted to the first  $2^d$ -ant, which is the same as in our model. (This restriction selects the 111... direction.) If the probability of any bond being occupied is  $p$ , for small  $p$  there are isolated clusters of connected sites, while above a threshold probability,  $p_c$ , there is an infinite directed cluster spanning the entire system.

A variant of conventional directed percolation is directed invasion percolation,<sup>16,17</sup> where one has a lattice in which all directed pairs of nearest neighbors are connected by bonds of varying preassigned strengths. Fluid is initially deposited at some site in the lattice, or along the top row. At every (discrete) time step, the occupied cluster grows by breaking the weakest (directed) bond on its surface, resulting in a new connection. In the large cluster limit, the occupied cluster has statistical properties which are essentially the same as the incipient spanning cluster that connects one end of the system to another at  $p_c$  in simple directed percolation.<sup>35</sup>

For  $p \lesssim p_c$ , one can define characteristic cluster lengths and masses, and obtain their scaling forms. The number of clusters of mass  $s$  (per unit volume) scales with the form

$$n_s(p) \sim s^{-\theta} Y(s^\sigma |p - p_c|); \quad (5.2)$$

comparing with our definitions, Eqs. (3.6) and (2.5), we see that

$$\theta - 2 = \frac{\kappa}{d_f} \quad (5.3)$$

and

$$\sigma = \frac{1}{d_f \nu}, \quad (5.4)$$

where we have taken  $p_c - p$  to be analogous to  $F_T - F$ . The mean-field values we obtain for these exponents,  $\theta = 5/2$  and  $\sigma = 1/2$ , turn out to be the same as obtained in mean-field theory for both isotropic<sup>14,15</sup> and directed percolation.<sup>17</sup> The correlation length exponent and fractal dimension of our system are, however, *different* from the corresponding exponents in directed percolation.

In addition, in contrast to conventional percolation, some of the exponents of our system are different on the two sides of the transition. This arises from the fact that the shape of the river network and correlation lengths above threshold are generated by river splits, which have no analogue below threshold. However, the exponent identities that we have obtained below threshold, which arise from simple scaling arguments, are similar to those for directed percolation. (Since the *definition* that we have for the polarizability is different from a conventional susceptibility, the relation between  $\gamma$  and the other exponents is different in our case.) The hyperscaling like relation,  $d_f + \kappa = (d + 1)/2$ , which is valid at and *below* the upper critical dimension, is also the same as in directed percolation,<sup>17</sup> expressing the fact that the number of clusters of length  $\sim \xi$  in a correlation volume is  $O(1)$ , independent of the distance to the threshold.

The primary difference between our results below threshold and standard directed percolation in mean-field theory is the difference in the way in which the clusters grow, which affects  $\nu$ , the correlation length exponent, as well as the shapes of the clusters, parametrized by  $d_f$ . The qualitative picture that we have is of clusters growing in a kind of “runaway” process, with  $d\xi/dF$  for the same (large)  $\xi$  being greater than for standard percolation. This would suggest that our value for  $\nu$  should be greater than in standard percolation (although the difference could have been irrelevant, leaving  $\nu$  unchanged). In normal directed percolation,  $\nu = 1$  and  $\nu_\perp = 1/2$  in mean-field theory, in contrast to our values of  $\nu = 3/2$  and  $\nu_\perp = 3/4$ . The larger correlation length exponents in our case result in a much lower upper critical dimension in our model; in standard directed percolation,  $d_c = 5$ , while  $d_c = 3$  in our system. Above the upper critical dimension,  $d_f = 2$  and  $\kappa = 3 - d_f = 1$  for directed percolation, in contrast to our results  $d_f = 4/3$  and  $\kappa = 2 - d_f = 2/3$ . Thus our clusters are longer and “stringier.” Below the upper critical dimensions, it is not very useful to compare the exact values of our exponents with the results for directed percolation, beyond the scaling laws relating various exponents noted above.

A variation of directed invasion percolation, which

is perhaps slightly closer to our model below threshold, has recently been considered by de Arcangelis and Herrmann.<sup>36</sup> They consider invasion percolation on a two-dimensional lattice, with the strength of the bonds between the sites growing weaker (with a power-law falloff) as one proceeds further from the initial cluster in which fluid is present. This makes already large clusters more likely to grow further, as in our system. The initial cluster is in the middle of the system, and the invasion process is stopped when the cluster reaches the boundary of the system. Because it is necessary to stop the growth after a finite time, the shape of the cluster that they obtain is a *nonequilibrium* property. This is in contrast to our system, where there is a controllable external force, as a function of which we study the *equilibrium* shape of the clusters. Even with the nonequilibrium approach of de Arcangelis and Herrmann, however, the distribution of sites in the invaded cluster is found to be consistent with a simple scaling form, with a fractal dimension of  $1.29 \pm 0.03$ . This fractal dimension appears to be independent of the exponent in the power-law falloff of the bond strengths, and is fairly close to the value of  $d_f$  we have obtained in two dimensions.<sup>37</sup> Whether this similarity is more than a coincidence, we leave as an open question.

Above threshold, if we use the current driven version of our model, it is qualitatively related to various river network models that have been considered by previous authors. Kramer and Marder<sup>38</sup> have analyzed a model for flowing rivers that allows for erosion of the landscape. This alters the shape of the river network qualitatively, *dynamically* eliminating the river splits in the long time limit by *deepening* the channels. While erosion is undoubtedly crucial in understanding real river systems in nature, our model, which can be viewed as fluid flowing over a “rocky” surface, is more appropriate to problems involving materials with quenched disorder.

Takayasu and Huber<sup>39</sup> have considered models with quenched randomness, in which the rivers are not allowed to split. Thus, unlike in our model, the channels get fuller as one progresses downhill, with a steady “rain” of fluid preventing them from becoming sparse. Although there is no thermodynamic limit in the strict sense, a scale invariant probability distribution for the channel currents is found, which scales as  $P(J) \sim J^{-\tau}$ . The exponent  $\tau$  is  $4/3$  in 1+1 dimensions, and  $3/2$  in mean field. (The first moment of the distribution diverges because of the steady rain.) It is not clear if one can make meaningful comparisons with our model, where scale invariance exists only at the critical point and the extra physics of river splits is essential.

## VI. APPLICATIONS AND CONCLUSIONS

The model that we have presented here is potentially applicable either directly or at least qualitatively to a variety of physical systems. The most direct application is to the problem we have modeled: fluid on a tilted two-dimensional irregular or chemically dirty surface. Our results, up to the caveats in the previous section, should

be directly applicable. A related three-dimensional problem is gravity driven invasion of a nonwetting fluid into a porous material. If fluid is not present in the system initially, but only enters through the top boundary, there will be no isolated clusters below threshold; however, the scaling properties of clusters connected to the top boundary can be studied as a function of the driving force (perhaps overall tilt in an anisotropic medium). There would seem to be two rather different regimes. If the fluid remains collected in small droplets within the medium, which break and spill into lower regions when they get too large or when the force on them exceeds a critical value, then, qualitatively, the present model should apply with the “lakes” representing the droplets. The main complication below threshold is the possible “overshooting” when a saturated droplet breaks, since this will leave it unsaturated. Above threshold, the system can be current driven, and the ratios of exponents, e.g.,  $\beta/\nu$ , measured. The effects of capillarity, the discrete breaking of droplets, and viscous pressure gradients must be analyzed to make concrete predictions. In particular, it is not clear whether there will be a well-defined analog of the microscopic exponent  $\beta_0$ .

A very different regime will exist if the invading fluid remains *connected* rather than breaking into droplets. In this case the pressure at the bottom of a cluster will be proportional to its vertical length in static equilibrium, and therefore well away from the top will exceed any capillary forces that stop the cluster from growing. In this case, the growth will be very different—probably dominated by rare regions—and the model will not be applicable. This is because of the failure of one of the essential features of our model is the *uniform* external driving field in the direction of the transport. Thus it will also not be applicable to the case of *pressure* driven fluid invasion into a porous medium.<sup>5–8</sup> In this case, when the fluid can be approximated as being in static equilibrium, there is *constant* pressure throughout a cluster, and all weak barriers at the boundary of the cluster are equally likely to rupture, irrespective of their location, corresponding to standard (isotropic) invasion percolation.<sup>6,7</sup> At finite velocities, there is a drop in the pressure at sites distant from the driving source owing to viscous losses.<sup>8</sup> However, this *disfavors* the cluster from extending at its farthest extremity, in contrast to our model.

Another system for which our model might be qualitatively applicable is a two-dimensional type-II superconducting film, with vortices produced by an external magnetic field perpendicular to the film. (Since the transport carriers in our model are assumed to be pointlike, it will not be applicable to the case of flux lines in three dimensions.) In the absence of impurities, the vortices will be arranged in an Abrikosov lattice. If an electric current is passed through the sample in one of the directions in the plane, there is a gradient in the density of flux lines set up in the transverse direction, which causes a force on the flux lines along this gradient. The entire lattice moves collectively, and the transport that of an elastic medium, related elastic systems have recently been analyzed extensively.<sup>12</sup> If there is strong impurity-induced disorder in the sample, the lattice structure is destroyed,

and at very low temperatures where thermal fluctuations are small, the system will be in a “vortex glass” phase.<sup>4</sup> The external current will then no longer produce a uniform force, but rather a spatially varying one which is determined by the impurity and vortex locations.<sup>3</sup> This is more similar to the random surface that we have looked at here, where there is an overall downward slope due to the external tilt, which is then modified by local variations in the surface height. However, as we shall see, there are various complications.

Flux flow can be measured in superconductors from the  $I$ - $V$  characteristics in the vicinity of the critical current. Spatial inhomogeneities in the transport could perhaps be measured using SQUIDS with small pickup coils.<sup>40</sup> Below threshold,  $ac$  response measurements could be used to find the polarizability.

A similar system to the flux lattice is an array of magnetic bubbles; these occur in certain two-dimensional films magnetized perpendicular to the film, where small domains of opposite magnetization are created.<sup>41</sup> These bubbles can be pinned by impurities, like the vortices in a superconductor, and driven by a magnetic field gradient or other means. For magnetic bubble systems, measurements can be made directly by imaging the bubbles.

As mentioned in the discussion on boundary conditions in Sec. V, the method of generating the external force by gradients in the density prevents one from going to the large system limit in both of these cases; the range of size (if any) for which the picture discussed in this paper is applicable will depend on the parameters of the system. The *discrete* nature of the vortices (and bubbles), as opposed to the continuum fluid that we have been considering here, causes additional complications, possibly more severe than the effects of breaking droplets mentioned above. When the vortex creep is very small, individual vortices hop forward one by one, rather than in a smooth stream. The form of the local current can thus not be represented by a continuum approximation. More seriously, the vortex distribution in the sample will now no longer be constant in time, but have temporal fluctuations. It may thus be more appropriate in this regime to treat the system as a directed quenched “sandpile,”<sup>33</sup> with the discreteness playing an important role. There is, however, a limit where our model may be applicable: if the length scales of the variations of the film composition (or thickness) are large compared to the vortex spacings, and the temperature is high enough that thermal fluctuations cause the current leaving each “lake” to be stochastically independent of other lake outlets, but low enough that the typical outlet barriers in unsaturated lakes are much larger than  $k_B T$ , then the continuum fluid model should be appropriate. The discreteness of the vortices would then be like the discreteness of water molecules in the fluid flow problem. This regime may well be obtainable in superconducting films, that are strongly inhomogeneous on mesoscopic scales.

There are also other systems that are qualitatively similar to the model presented here, although the connections will be much harder to establish. One of these is charge-density waves (CDW’s) in an *insulator*<sup>9</sup> in the presence of strong disorder, although it is not clear

whether such strong disorder is compatible with a classical description of the dynamics. In addition, there is no conservation of CDW charge, since CDW current can be transformed into normal current. Although this effect might be small for poor conductors, it will probably destroy the sharpness of the threshold. The long range Coulomb interactions are an additional complication. Another system that one might study is dielectric breakdown in an insulator,<sup>11</sup> but again the long range Coulomb force between the charges will change the behavior dramatically, unless it is well screened, in which case models like the one we have considered here may be applicable.

## VII. SUMMARY

In this paper, we have considered a novel class of collective transport phenomena involving driven fluid or plastic flow in disordered media. A key feature of the model and the potential applications discussed in this section is the nonlocal nature of the transport: the clusters below threshold and the current paths above threshold are determined by far away parts of the system, in a much stronger way than for conventional percolation. We have found various unusual features within a simple model, including different scaling laws above and below threshold. Many features of the model need to be analyzed in greater detail; for instance, the effects of thermal noise, finite size effects, transients, the modifications produced in continuum systems instead of lattice models and, perhaps most crucially, the effects of discrete carriers. The model that we have constructed and the analysis we have carried out are really a starting point; much more work is clearly required to make concrete connections with most of the broad variety of systems to which similar models might be applicable.

## ACKNOWLEDGMENTS

We thank B. I. Halperin, J. T. Chayes, and L. Chayes for useful discussions. This work was supported by the NSF via Grant No. DMR 9106237 and the Materials Research Laboratory at Harvard University. D.S.F. was supported by the A.P. Sloan Foundation. The hospitality of the Institute for Theoretical Physics at Santa Barbara, where some of this work was carried out by DSF, is also gratefully acknowledged.

## APPENDIX A: ONE DIMENSION AND LOCAL CURRENT LAWS

In this appendix, we analyze the one-dimensional continuum system in some detail. In addition to understanding the behavior for  $d = 1$ , this is useful to motivate the lattice model we construct in the main text, in particular, the local current law Eq. (2.3) which is discussed at the end of this appendix.

Figure 2 shows the distribution of fluid for a typical realization of the randomness in one dimension. For any value of the tilt  $F$ , by proceeding up from the downhill end of the system it is possible to obtain the capacity of the different lakes in the system. The total capacity of

all the lakes together represents the maximum amount of fluid that can be poured in at that value of  $F$  before current flows across the system. If  $h(x)$  is the depth of the fluid layer as a function of the position,  $x$ , this can be used to define an  $\bar{h}_T(F)$  for large systems, which is the mean density of fluid the system contains at threshold;  $\bar{h}_T(F)$  is a smooth function of  $F$ , and can thus be assumed to be linear over any small range of  $F$ . The function  $\bar{h}_T(F)$  can be inverted, to obtain the threshold force  $F_T(\bar{h})$ , as a function of a prescribed mean density of fluid,  $\bar{h}$ .

If we start with some random distribution of  $h$  in the system and start to increase the tilt  $F$ , the initial distribution will not be the same as that which would lead to all the lakes being filled to capacity at  $F = F_T(\bar{h})$ . Some regions will be disproportionately depleted, while others will have too much fluid in them. However, for a sufficiently large system, the threshold will still be at  $F_T(\bar{h})$ . This is because if the system is tilted beyond  $F_T$ , fluid will pour into any region from *all* the regions further uphill. For large systems, this will overwhelm the effect of any initial fluctuations in the distribution of fluid (apart from in a region close to the top). Conversely, below  $F_T$ , fluid from any region that initially has an excess can be absorbed into the whole downhill part of the system. This averages out the initial fluctuations, except close to the bottom. In Appendix B, where we consider lattice models below threshold with a particular choice for the distribution of the irregularities of the surface, the value of the threshold field that we obtain in one dimension is found to agree with this argument, i.e., it is the field at which all the fluid is just enough to saturate all the lakes.

We first examine the behavior above  $F_T$  and obtain a local equation for the current  $J(x)$  for a fluid governed by Newtonian viscosity. Let  $x$  and  $y$  be the horizontal and vertical coordinates, and  $h(x)$  be the height of fluid above the surface. For small  $h$ , with  $dh/dx \ll 1$ , the velocity gradients that are largest are the vertical gradients of the horizontal velocities,  $\partial_y v_x$ . We shall neglect all other velocity gradients. We also assume that fluid velocities are small, so that the dominant contribution to pressure gradients comes from variations in  $h(x)$ . The boundary conditions on the horizontal velocity are  $v_x(0) = 0$  and  $\partial v_x / \partial y|_{y=h(x)} = 0$ , which yields an approximately parabolic velocity profile along  $y$ . From this, it is possible to obtain the approximate current equation (suppressing constants like the coefficient of viscosity and density of the fluid),

$$J(x) = \int_0^{h(x)} v(y) dy \sim h^3(x) \left[ F(x) - \frac{dh(x)}{dx} \right]. \quad (\text{A1})$$

If the underlying physical forces governing the system are not like fluid viscosity, in general this relation might be modified to something of the form

$$J(x) \sim h^n(x) \left[ F(x) - \frac{dh(x)}{dx} \right]. \quad (\text{A2})$$

We shall use the general form of Eq. (A2) here.

For a one-dimensional system the continuity equation is trivial, and in steady state it is necessary that  $J(x)$

should be independent of  $x$ . Below threshold,  $J = 0$ . Equation (A2) then implies that at any point either  $F(x) - dh(x)/dx = 0$  or  $h(x) = 0$ . The first of these possibilities corresponds to the lakes, and the second to the interspersed dry regions. For small  $J$ , we seek a steady state solution with shallow rivers connecting the lakes.

Even if such a steady state solution exists, it is not clear *a priori* that it will be appropriate for the system. In reality, when  $F$  is increased beyond  $F_T$ , fluid flows out of each lake, reducing the level of the lake until it returns to saturation. For any lake, if this occurs before it is replenished by fluid from the lake above, the flow will stop temporarily in that region. If these breaks in the flow were frequent, the current flowing out from the system would be intermittent, and the steady state solution we seek here would not be relevant. However, we shall see that the probability of such events approaches zero as  $F \rightarrow F_T$ .

Equation (A2) is a first-order differential equation; at any value of  $J$  and  $F$ , there is a one-parameter family of solutions  $h(x)$ . However, for large systems, it is still possible to obtain a meaningful  $\bar{h}$ , which is the average of  $h(x)$  over  $x$ , as a function of  $J$  and  $F$  alone. To see this, consider two solutions  $h_1(x)$  and  $h_2(x)$  that satisfy the property  $h_1(x_0) > h_2(x_0)$  for some  $x_0$ . From Eq. (A2), it is then clear that the two solutions diverge from each other when integrated downhill. As long as  $h(x) > 0$  everywhere, as is necessary for  $J$  to be greater than zero, the difference between the two solutions will keep growing as we integrate downhill. Conversely, all solutions with a finite  $h(x_0)$  will converge towards each other as we integrate them uphill, and so as  $L \rightarrow \infty$ , as long as we choose a finite  $h(L)$ , the solution is uniquely determined (beyond a boundary region for  $x \approx L$ ). This also means that for a long river connecting two lakes,  $h(x)$  at the upper end can be obtained as a function of  $J$  (and vice versa), while  $h(x)$  at the lower end is not fixed by  $J$ .

Equation (A2) must now be solved to obtain  $h(x)$  as a function of  $J$ . At any fixed value of  $F$ , we can obtain  $\bar{h}$  as a function of  $J$ . Since  $\bar{h}_T(F)$  is linear in  $F$  for small changes in  $F$ , this yields the dependence of  $F - F_T(\bar{h})$  on  $J$  for fixed  $\bar{h}$ . Figure 15 shows the manner in which the system in the vicinity of a lake is divided into various regions. If  $h_0(x)$  is the depth of fluid as a function of  $x$  at threshold, we define  $h_1(x) = h(x) - h_0(x)$ . We approximate  $F(x) - dh/dx$  by  $F(x) - dh_0/dx \equiv F(x)$  in regions A and G, and by  $-dh_1/dx$  in B, C, D, and E. We also approximate  $h^n(x)$  by  $h_0^n(x)$  in region D, and  $h_1^n(x)$  in regions A, B, C, E, and G. (The first approximation is exact in regions C, D, and E, and the second in regions A, B, and G.) We thus obtain from Eq. (A2)

$$\begin{aligned} h_1^n(x)F(x) &= J \quad \text{in A and G,} \\ -h_1^n(x)\frac{dh_1(x)}{dx} &= J \quad \text{in B, C, and E,} \end{aligned}$$

and

$$-h_0^n(x)\frac{dh_1(x)}{dx} = J \quad \text{in D.} \quad (A3)$$

[Strictly speaking, Eq. (A2) is not valid in region D,

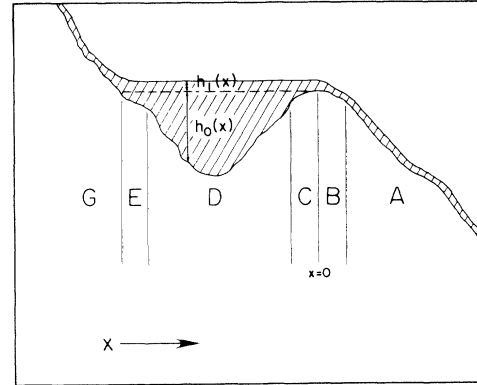


FIG. 15. Division of a section of a one-dimensional system above threshold into different regions. The dashed line is the actual capacity of the lake, while the hatched region is the actual distribution of the fluid. The widths of the regions B, C, and E shrink to zero as threshold is approached. The excess depth  $h_1(x)$  is almost constant in region D, decreasing only very slowly with increasing  $x$ .

where  $h(x)$  is large. However, the only property of Eq. (A3) for this region that we shall need is that it yields an approximately constant  $h_1(x)$ , which is correct.]

After linearizing  $F(x)$  around the lip of the lake, which is the boundary between regions B and C, Eq. (A3) can be solved by matching solutions in the different regions; the boundaries between regions are found by the requirement that  $h(x)$  and  $dh(x)/dx$  should be continuous. We find that as  $J \rightarrow 0$ , the width of the regions B and C vanishes, so that the linearization of  $F(x)$  around the lip of the lake is justified.

We also find that  $h_1(x) = O(J^{1/n})$  in the rivers, while  $h_1(x) = O(J^{2/(2n+1)})$  in the lakes, with a crossover between the two in regions like B, C, E, and G. Since the lakes occupy a finite fraction of the system, to leading order in  $J$  we obtain

$$\bar{h}_1(x) = O\left(J^{2/(2n+1)}\right) \quad (A4a)$$

which can be inverted to give

$$J \sim \bar{h}_1(x)^{n+\frac{1}{2}} \sim (F - F_T)^{n+\frac{1}{2}}. \quad (A4b)$$

Thus in Eq. (2.3), used to define the flow over barriers in the lattice model, the exponent  $\beta_0$  in one dimension is  $\beta_0 = n + \frac{1}{2}$ . One can also verify that the steady state solution is appropriate for the system: as  $J \rightarrow 0$ , the fraction of the excess fluid present in the rivers becomes infinitesimal, so that the probability of the flow ceasing temporarily tends to zero.

By the nature of the approximations made in Eqs. (A3), the  $h_1(x)$  that we have obtained is greater than the solution to the exact equation. Since  $F(x) > -dh(x)/dx$  in A and G and  $< -dh(x)/dx$  in B, while  $h_1 > h_0$  in C and E and  $< h_0$  in D, if we replace  $J$  with  $J/2$  for A, B, G and with  $J/2^n$  for C, D, and E in Eqs. (A3), we would obtain a solution  $h_1(x)$  that is everywhere less than the exact solution. This modified version of Eqs. (A3) can be solved as before, and leaves

the scaling of Eq. (A4a) unaltered, leading to the same value of  $\beta_0$  as above.

### 1. Polarizability

The behavior of the polarizability and polarization below threshold can also be ascertained for the one-dimensional system. In the continuum system, unlike in its lattice version, it is possible to define separate forward and backward polarizabilities; these are given by the change in the polarization upon a slight increase or decrease of the force  $F$ , respectively. The forward polarizability is defined even in the lattice model, and is obtained in Appendix B for  $d = 1$ . Here we evaluate the *backward* polarizability. Figure 16 shows the effect of reducing the force from  $F$  to  $F - dF$ . As can be seen, in most of the lakes this simply results in the fluid moving backwards slightly. The new surface of the lake is determined by the conditions that the amount of fluid in the lake does not change due to this reduction in the force, and that the slope of the surface is only a function of the external force. From Fig. 16, one can see that the total backward displacement of fluid in the typical lakes is  $O(dF)$ . The calculations are slightly different in “anomalous” lakes where the fluid spills out backwards from the lake and moves a finite distance. But since the fraction of such lakes is  $O(dF)$ , the total displacement of fluid from these lakes is also only  $O(dF)$ . This means that the backward polarizability *remains finite* upto  $F_T$ , and its absence in the lattice version is not of consequence. The forward polarizability is, however, singular, and is calculated within the lattice model in Appendix B.

### 2. Higher dimensions

In Sec. V, we have seen that, in higher dimensions, the local current flow Eq. (A2) is modified by factors of the width of the river, which depends on the depth of fluid in it. As a river proceeds downhill, its location in transverse

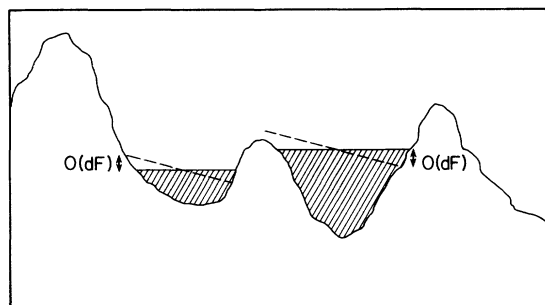


FIG. 16. Change in the polarization on reducing the force from  $F$  to  $F - dF$  in a one-dimensional system. The hatched regions show the lakes at  $F$ , the dashed lines show the way their levels try to adjust to the reduction of the force. The lake on the left has a reduction in polarization of  $O(dF)$ . The lake on the right is “anomalous,” in that some fluid pours out backwards from it when the force is reduced; the fraction of such lakes is  $O(dF)$ .

space is determined by the condition that the random potential should have a local minimum in the transverse directions. For small  $h(x)$ , with a generic quadratic saddle point for the random potential, this produces an extra factor of  $(\sqrt{h(x)})^{d-1}$  in Eq. (A2). [This condition is not valid far into the lakes, where  $h(x)$  is large; however, the scaling of the current is not controlled by the behavior in this region.] Thus the exponent  $n$  in Eq. (A2) is replaced by  $n + (d-1)/2$ , which modifies Eq. (A4), yielding  $\beta_0(d) = n + d/2$ . For the simple generalization of the viscous flow Eq. (A1), we have  $\beta_0 = 3 + d/2$ .

### APPENDIX B: MEAN-FIELD THEORY BELOW THRESHOLD

In this appendix, we analyze the behavior of our lattice model below threshold in mean-field theory and also in one dimension.

The mean-field model introduced in Sec. III is specified as follows: each site at the  $m$ th level from the top has one lowest outlet through which it can overflow to some particular site in the  $(m+1)$ th level, and some number  $r$  of inlets from the  $(m-1)$ th level with  $r$  varying randomly from site to site with probability  $c_r$  satisfying the condition that the mean number of inlets  $\sum_r r c_r = 1$ , which is the number of outlets from each site. Initially, a random depth of fluid  $h_i^0$  is put at each site, resulting in a depth above the lowest-outlet-barrier  $\min_\alpha b_{i\alpha}$  of

$$a_i \equiv h_i^0 + F - \min_\alpha b_{i\alpha} \quad (\text{B1})$$

with distribution  $A(a)$ . The system is then equilibrated as follows: the excess fluid on the sites (i.e.,  $a_i$  if  $a_i > 0$ ) in the top (zeroth) level is allowed to overflow over the lowest outlet to the first level, resulting in a new  $\{h_i\}$  in the first level sites, and height relative to the barrier

$$\Delta_i = h_i + F - \min_\alpha b_{i\alpha}. \quad (\text{B2})$$

This process is continued downwards, with a site  $i$  at the  $m$ th level overflowing to the  $(m+1)$ th level if  $\Delta_i$ , after it has received all the overflows from the uphill sites, is positive. The value of  $\Delta_i$  is thus given by Eq. (3.3),

$$\Delta_i = a_i + \sum_{k=1}^r \max[\Delta_{i_k}, 0] \quad (\text{B3})$$

with the sum running over the  $r$  inlets  $i_1, \dots, i_r$  to the site  $i$  from the previous level.

If a site overflows, it connects itself and the cluster of sites which have overflowed into it onto a cluster which includes its outlet site at the next level down. We define  $s_i$  as the mass that the overflow of the  $i$ th site adds to the cluster. For sites that do not overflow, and thus are at the terminus of clusters,  $s_i = 0$ . The cluster mass  $s_i$  thus satisfies the recursion relation given by Eq. (3.8),

$$s_i = 1 + \sum_k s_{i_k} \text{ for } \Delta_i \geq 0$$

and

$$s_i = 0 \text{ for } \Delta_i < 0. \tag{B4}$$

The crucial simplification in the mean-field limit with

random outlet connections from each level to the next is that we expect  $\Delta_i$  and  $s_i$  for all the sites in a given row to be *independent* in the limit of an infinite system. The convenient quantity to analyze is the joint distribution  $P_m(\Delta; s)d\Delta$  of  $\max[\Delta, 0]$  and  $s$ , so that  $P_m$  has a  $\delta$  function at  $\Delta = 0$  and  $s = 0$  corresponding to the sites that do not overflow. The recursion relation for  $P_{m+1}$  is then given by Eq. (3.9),

$$P_{m+1}(\Delta; s) = \sum_{r=0}^{\infty} c_r \prod_{j=1}^r \left[ \int d\Delta_j \sum_{s_j} P_m(\Delta_j; s_j) \right] A \left( \Delta - \sum_j \Delta_j \right) \delta_{s, 1+\Sigma s_j} - \hat{\mu}_m(\Delta; s) + \delta_{s,0} \delta(\Delta) \sum_{s'=1}^{\infty} \int_{-\infty}^0 d\Delta' \hat{\mu}_m(\Delta'; s'), \tag{B5}$$

where the function  $\hat{\mu}_m(\Delta; s)$  which vanishes both for  $\Delta > 0$  and for  $s = 0$  cancels the part of the first term in the equation with  $\Delta < 0$ , and the third term replaces this by a  $\delta$  function at  $\Delta = s = 0$ , corresponding to the unsaturated (nonoverflowing) sites. In terms of the Fourier transform,

$$P_m(\omega; s) = \int_{-\infty}^{\infty} d\Delta P_m(\Delta; s) \exp(i\omega\Delta), \tag{B6}$$

and similarly for  $\hat{\mu}$ , the evolution of  $P_m$  is then given by

$$P_{m+1}(\omega; s) = \left\{ \sum_{r=0}^{\infty} c_r \prod_{j=1}^r \left[ \sum_{s_j} P_m(\omega; s_j) \right] \times A(\omega) \delta_{s, 1+\Sigma s_j} \right\} - \hat{\mu}_m(\omega; s) + \delta_{s,0} \sum_{s'=1}^{\infty} \hat{\mu}_m(\omega = 0; s'). \tag{B7}$$

As discussed in Sec. III,

$$\mu_m(s) = \int d\Delta \hat{\mu}_m(\Delta; s) \tag{B8}$$

is the density of clusters of mass  $s$  that terminate at the  $m$ th row from the top of the system.

For a general  $A(a)$ , it is not at all clear how to solve Eq. (B7). One could try to *guess* a form for  $\hat{\mu}_m(\Delta; s)$ , and verify that it yields a  $P_m(\Delta; s)$  that is zero for  $\Delta < 0$ . This requires guessing a whole function, which involves an infinite number of parameters. However, if we consider the special class of functions  $A(a)$  which decay exponentially for  $a < 0$ , the first term of Eq. (3.9) must generate functions that *also* decay exponentially for  $\Delta < 0$ . This is because every  $P_m(\Delta_j; s_j)$  in Eq. (3.9) shifts the distribution  $A(a)$  towards larger values of  $a$ , which preserves its exponential form for  $a < 0$ . This implies that the correction terms  $\hat{\mu}_m(\Delta; s)$  in Eq. (3.9) are also exponential in  $\Delta$  for each  $s$ , decaying at the same rate as  $A(a)$  for  $a < 0$ . Thus only the *strengths* of the exponentials for each  $s$  need to be determined self-consistently. For simplicity

of later calculations, we choose  $A(a)$  to be exponentially decaying for  $a > 0$  as well, and continuous across  $a = 0$ , as given in Eq. (3.11), which has the Fourier transform

$$A(\omega) = \frac{1}{g+1} \left\{ \frac{g}{1-ig\omega} + \frac{1}{1+i\omega} \right\}. \tag{B9}$$

As discussed in Sec. III, threshold is reached by increasing  $g$ , and close to threshold

$$\epsilon \equiv g_T - g \propto F_T - F. \tag{B10}$$

We discuss other forms of  $A(\omega)$  later in this appendix.

For the distribution in Eq. (B9),  $\hat{\mu}_m(\omega; s)$  must have the form

$$\hat{\mu}_m(\omega; s) = \frac{\mu_m(s)}{1+i\omega}. \tag{B11}$$

Below threshold, for large  $m$  the distribution functions should be independent of  $m$ . Thus we look for a fixed point to the recursion relation Eq. (B5). In terms of the generating functions

$$P(\omega; y) = \sum_{s=0}^{\infty} y^s P(\omega; s) \tag{B12}$$

and

$$\mu(y) = \sum_{s=1}^{\infty} y^s \mu(s), \tag{B13}$$

we obtain the fixed point equation, Eq. (3.14),

$$P(\omega; y) = \sum_{r=0}^{\infty} c_r y A(\omega) [P(\omega; y)]^r + \mu(y=1) - \frac{\mu(y)}{1+i\omega}. \tag{B14}$$

The threshold  $F_T$  is found by increasing  $g$  in Eq. (B9) until there is no physical solution  $P(\omega; y)$  to this fixed point equation.

We must still chose the probabilities  $c_r$  of the number of inputs. In the hope that different choices for the

constants  $c_r$  in Eq. (B14) will not affect the mean-field nature of the solution, so long as we allow inputs to a site from more than one site (i.e., not all  $c_r$ 's with  $r > 1$  are equal to zero) we choose

$$c_0 = \eta, \quad c_1 = (1 - 2\eta), \quad \text{and } c_2 = \eta \quad (\text{B15})$$

with  $0 \leq \eta \leq \frac{1}{2}$ . This satisfies the constraints mentioned earlier,  $\sum c_r = 1$  and  $\sum r c_r = 1$ , for all values of  $\eta$ . The special case of  $\eta = 0$ , where  $c_r = \delta_{r,1}$ , corresponds to each site being linked to exactly one site in the next row, and therefore represents a one-dimensional system. More general choices for the  $c_r$ 's will be discussed later. For the choice of  $c_r$ 's in Eq. (B15), Eq. (B14) is a quadratic in  $P(\omega; y)$ , and can be solved. For the case of  $d = 1$ , it reduces to a linear equation.

### 1. One-dimensional case

We first solve Eq. (B14) for the simple one-dimensional case. It is useful to first consider Eq. (B14) for  $y = 1$ ; we denote  $\mu(y = 1)$  by  $\mu$ . This corresponds to ignoring the dependence of the distributions on  $s$ . Equation (B14) then reduces to

$$P(\omega) \equiv P(\omega; y = 1) = A(\omega)P(\omega) + \mu \left\{ 1 - \frac{1}{1 + i\omega} \right\} \quad (\text{B16})$$

with  $A(\omega)$  given by Eq. (B9). The solution to this is

$$P(\omega) = \frac{\mu(1 - ig\omega)}{1 - g - ig\omega}. \quad (\text{B17})$$

The normalization condition,  $P(\omega = 0) = 1$ , yields

$$\mu = 1 - g. \quad (\text{B18})$$

This corresponds to the distribution

$$P(\Delta) = (1 - g)\delta(\Delta) + (1 - g) \exp[-(1 - g)\Delta/g]. \quad (\text{B19})$$

Threshold is reached at  $g = 1$ ; for  $g > 1$ , the solution Eq. (B19) diverges at large  $\Delta$  and is unphysical. This is a special case of the more general argument presented in Appendix A, that threshold for one-dimensional systems occurs when the amount of fluid in the system is equal to its "capacity" which is equivalent for the lattice model to the condition that the first moment of  $A(a)$  should vanish. This indeed occurs at  $g = 1$ . For  $g \lesssim 1$ , Eq. (B19) becomes

$$P(\Delta) = \epsilon \{ \delta(\Delta) + \exp[-\epsilon\Delta] \}, \quad (\text{B20})$$

where  $\epsilon = 1 - g$ . As discussed in Sec. III, the singular part of the polarization density is given by

$$\Pi_s = \int_0^\infty d\Delta P(\Delta)\Delta. \quad (\text{B21})$$

From Eq. (B20), we have  $\Pi_s \sim 1/\epsilon$ , from which

$$\gamma = 2. \quad (\text{B22})$$

We now consider Eq. (B14) for  $P(\omega; y)$  for general  $y$  in one dimension. From Eq. (B14), we have

$$P(\omega; y) = yA(\omega)P(\omega; y) + \mu(y = 1) - \frac{\mu(y)}{1 + i\omega}. \quad (\text{B23})$$

$P(\omega; s)$  can be found from  $P(\omega; y)$  by integrating over the unit circle  $|y| = 1$ :

$$P(\omega; s) = \frac{1}{2\pi i} \oint \frac{dy}{y^{s+1}} P(\omega; y). \quad (\text{B24})$$

One can deform the contour so that only the singularities of  $P(\omega; y)$  contribute.

Equation (B23) has the solution

$$P(\omega; y) = \frac{(1 + i\omega)\mu(y = 1) - \mu(y)}{1 + i\omega - y/(1 - ig\omega)}. \quad (\text{B25})$$

As we have seen already,  $\mu(y = 1) = 1 - g$ . The denominator of Eq. (B25) has a zero with  $\text{Im}(\omega) > 0$ . This has to be cancelled by a zero in the numerator, otherwise transforming back to  $\Delta$  would yield  $P(\Delta)$  with support for  $\Delta < 0$ . This condition gives us an equation for  $\mu(y)$ ,

$$\mu(y) = (1 - g) \frac{1 + g - \sqrt{4(1 - y)g + (1 - g)^2}}{2g}. \quad (\text{B26})$$

This satisfies the conditions  $\mu(y = 1) = 1 - g$ , and  $d\mu(y)/dy|_{y=1} = 1$ , required by the normalization condition  $\sum s\mu(s) = 1$ .

As mentioned earlier, the function  $\mu(s)$  is simply the probability that a cluster of length  $s$  terminates at some site, so that it gives the distribution of cluster sizes. For  $g \lesssim 1$ ,  $\mu(y)$  has a square root branch cut at  $y = 1 + \epsilon^2/4$ . Inverting Eq. (B26), as in Eq. (B24), the scaling form of  $\mu(s)$  is controlled by the origin of the branch cut in  $\mu(y)$ , and for small  $\epsilon$  is of the form

$$\mu(s) \sim \frac{\epsilon}{s^{3/2}} \exp[-\epsilon^2 s/4], \quad (\text{B27})$$

valid for small  $\epsilon$  and large  $s$ , for any value of the scaling variable  $\epsilon^2 s$ . The characteristic length of a cluster is thus  $\sim 1/\epsilon^2$ , which implies

$$\nu = 2. \quad (\text{B28})$$

From the scaling of  $s\mu(s)ds$ , we obtain for the exponent of the fraction of sites in clusters of size  $\xi$ ,

$$\kappa = 0, \quad (\text{B29})$$

as expected, since in one dimension all the sites are connected above threshold. Comparing with Eq. (B22), we see that the scaling law  $\gamma = \nu(1 - \kappa)$  is satisfied.

### 2. Mean-field limit

We now solve Eq. (B14) for the mean-field limit, with  $\eta \neq 0$  in Eq. (B15). The specific case of  $\eta = \frac{1}{4}$  is alge-

braically the simplest, and we specialize to this. Again, as in the previous subsection, we first consider the case of  $y = 1$ , i.e., ignoring cluster masses. From Eq. (B14), with  $\mu = \mu(y = 1)$ , we have

$$P(\omega) = \frac{1}{4}A(\omega)[1 + P(\omega)]^2 + \mu \left\{ 1 - \frac{1}{1 + i\omega} \right\}. \quad (\text{B30})$$

This is quadratic in  $P(\omega)$ , and can be solved, yielding

$$P(\omega) = -1 + 2(1 - ig\omega) \left\{ 1 + i\omega \pm \sqrt{(1 + i\omega)^2 - (1 + i\omega + i\mu\omega)/(1 - ig\omega)} \right\}. \quad (\text{B31})$$

The consistency condition to be used to determine  $\mu$  is more subtle than for  $d = 1$ . The discriminant in Eq. (B31) always vanishes at  $\omega = 0$ , so that  $P(\omega)$  generically has a square-root branch cut at  $\omega = 0$ , which we can choose to lie along the negative imaginary axis. Such a branch cut would lead to a  $P(\Delta)$  decaying as a power law,  $\sim \Delta^{-3/2}$ , for large  $\Delta$ . However, the fixed point solution Eq. (B31) to Eq. (B30) has been obtained without reference to the initial condition that  $P_m(\Delta)$  starts out at  $m = 0$  without any such power-law tail. Below threshold, where the clusters are finite, we do not expect a long tail to *build up* in the distribution as we increase  $m$ . Thus to obtain the physically appropriate solution,  $\mu$  has to be adjusted so as to create a *double* root in the discriminant at  $\omega = 0$  in Eq. (B31), and thereby eliminate the branch cut. The desired value of  $\mu$  is the same as Eq. (B18). Substituting this in Eq. (B31), we obtain

$$P(\omega) = -1 + 2(1 - ig\omega) \left\{ 1 + i\omega - i\omega \sqrt{(1 - 2g - ig\omega)/(1 - ig\omega)} \right\}. \quad (\text{B32})$$

The sign of the square root has been chosen to give  $P(\omega) = 1$  for  $g = 0$ , when the entire distribution  $A(a)$  is located to the left of the origin. One can carry out the analysis for a general choice of  $\eta$  in Eq. (B15), and the behavior is qualitatively similar. If we vary  $\eta$  continuously from  $\frac{1}{4}$  to zero, the solution analogous to Eq. (B32) transforms into the one-dimensional solution, Eq. (B17).

The fixed point function  $P(\omega)$  has a branch cut at  $-i(1 - 2g)/g$ , which lies on the negative imaginary axis for small  $g$ . This produces an exponentially decaying function  $P(\Delta)$ , with a power-law prefactor. As  $g$  is increased, this branch cut moves in, until at  $g = g_T = \frac{1}{2}$ , we again have a branch cut starting at  $\omega = 0$ , which yields distributions with power-law tails. For  $g = \frac{1}{2}(1 - \epsilon)$ , the scaling form of  $P(\Delta)$  can be found from Eq. (B32) to be

$$P(\Delta) \sim (4\epsilon\Delta + 3) \exp[-2\epsilon\Delta]/\Delta^{\frac{5}{2}} \quad (\text{B33})$$

for small  $\epsilon$ , large  $\Delta$ , and arbitrary  $\epsilon\Delta$ . Although the general form for  $P(\Delta)$  for small  $\Delta$  is complicated, it is easy to see that  $P(\Delta) \geq 0$  for all  $\Delta$ . The strength of the branch cut is positive along its entire length, as is the weighting factor of  $\exp[-i\omega\Delta]/(2\pi)$  used to evaluate  $P(\Delta)$ , so the resulting  $P(\Delta)$  is positive. At threshold,

$g = \frac{1}{2}$ , the branch cut in  $P(\omega)$  is of the form  $\omega^{3/2}$ , from which

$$P(\Delta) \sim 1/\Delta^{5/2}. \quad (\text{B34})$$

This scales in the same way as Eq. (B33). As for  $d = 1$ , one can obtain  $\gamma$  by calculating the polarization,  $\int d\Delta [\Delta P(\Delta)]$ . The singular part of this close to threshold arises from the asymptotic form of  $P(\Delta)$ . From Eq. (B33),  $\Pi_s = 1 - O(\epsilon^{\frac{1}{2}})$ , so that

$$\gamma = 1/2. \quad (\text{B35})$$

One can also obtain the distribution of cluster sizes as in one dimension, by considering the general form of Eq. (B14) for arbitrary  $y$ . With the choice of  $\eta = 1/4$  in Eq. (B15), we have

$$P(\omega; y) = \frac{1}{4}yA(\omega)[P(\omega; y) + 1]^2 + \mu(y = 1) - \frac{\mu(y)}{1 + i\omega}. \quad (\text{B36})$$

This is quadratic in  $P$ , and can be solved. The singularities in  $P(\omega; y)$  are in the discriminant of this solution, which is

$$D = (1 + i\omega)^2(1 - ig\omega) - y[(2 - g)(1 + i\omega) - \mu(y)], \quad (\text{B37})$$

where we have used the earlier result  $\mu(y = 1) = 1 - g$ .

The discriminant  $D$  is cubic in  $\omega$ . For  $y = 1$ , this is the same as our result in Eq. (B31). [We have included a factor of  $1 - ig\omega$  inside the discriminant in Eq. (B37).] The discriminant then has a double root at  $\omega = 0$ . If we change  $y$  smoothly from 1, the double root will generically split into two roots which move away continuously from  $\omega = 0$ . Since the roots of the discriminant control the exponential damping of  $P(\Delta; s)$ , this would lead to  $P(\Delta; s)$  decaying much more slowly than  $P(\Delta) = \sum_s P(\Delta; s)$ , which is unphysical. We therefore have to adjust  $\mu(y)$  so that the discriminant has a double root for all  $y$ . This yields a condition that is quadratic in  $\mu(y)$ . The function  $\mu(y)$  is generally smooth for  $y$  near one, but has singularities which come from the discriminant of the quadratic equation which yielded  $\mu(y)$ :

$$D_\mu = 16y^2[(1 - 2g)^2 + (3g^2 - 6g)(y - 1)]^3. \quad (\text{B38})$$

This has a branch cut that moves into  $y = 1$  as  $g \rightarrow 1/2$ . For  $g = 1/2 - \epsilon$ , the scaling form for  $\mu(s)$  that this yields is

$$\mu(s) \sim \frac{1}{s^{5/2}} \exp[-16\epsilon^2 s/9] \quad (\text{B39})$$

valid for small  $\epsilon$ , large  $s$  and any  $\epsilon^2 s$ . The probability of being in a cluster of size  $s$  scales as  $s\mu(s)ds$ . From Eq. (3.1), with  $s \sim l^{d_f}$ , we thus have

$$\frac{\kappa}{d_f} = \frac{1}{2}. \quad (\text{B40})$$

Also, from the decay of the exponential in Eq. (B39),

since  $\epsilon \sim |f|$ , we have

$$d_f \nu = 2 \quad (\text{B41})$$

which, when combined with Eq. (B40), gives

$$\kappa \nu = 1. \quad (\text{B42})$$

### 3. Correlation length

Unlike the case in  $d = 1$ , in higher dimensions the length  $l$  and the mass  $s$  of a cluster are different. If one tries to obtain a distribution function  $P(\omega; l)$  analogous to  $P(\omega; s)$ , the evolution equation cannot be expressed simply in terms of generating functionals. This is because when two sites  $i_1$  and  $i_2$  feed into a site  $i$  at the next row, we have  $l_i = 1 + \max\{l_{i_1}, l_{i_2}\}$  instead of the simple addition law for cluster masses. We have not been able to solve the resulting equations directly. We therefore obtain the correlation length indirectly.

If we add a small extra amount of fluid to the sites in a particular level, the typical distance that this extra fluid flows down will be the characteristic cluster length. This is equivalent to perturbing  $P(\omega)$  around its fixed point form, and examining the approach back to the fixed point. A small perturbation  $\delta P(\omega)$  evolves as

$$\begin{aligned} \delta P_{m+1}(\omega) &= \frac{1}{2} A(\omega) [1 + P(\omega)] \delta P_m(\omega) \\ &+ \delta \mu_m \left\{ 1 - \frac{1}{1 + i\omega} \right\} \end{aligned} \quad (\text{B43})$$

with the perturbation  $\delta P_0(\omega)$  specifying an initial condition for Eq. (B43). Here  $\delta \mu_m$  is related to the change in the number of clusters that terminate at the  $m$ th row. Transforming to

$$\delta P(\omega; z) = \sum_{m=0}^{\infty} z^m \delta P_m(\omega), \quad (\text{B44})$$

and  $\delta \mu(z) = \sum_{m=0}^{\infty} z^m \delta \mu_m$ , we have

$$\begin{aligned} \delta P(\omega; z) &= \delta P_0(\omega) + \frac{1}{2} z A(\omega) [1 + P(\omega)] \delta P(\omega; z) \\ &+ z \delta \mu(z) \left\{ 1 - \frac{1}{1 + i\omega} \right\}. \end{aligned} \quad (\text{B45})$$

This can be solved to give

$$\delta P(\omega; z) = \frac{\delta P_0(\omega)(1 + i\omega) + i\omega z \delta \mu(z)}{1 + i\omega - \frac{1}{2} z [1 + P(\omega)] / (1 - ig\omega)}. \quad (\text{B46})$$

Since

$$\delta P_0(\omega) = \oint \frac{dz}{2\pi iz} \delta P(\omega; z), \quad (\text{B47})$$

Eq. (B46) can be used to obtain  $\delta \mu(z)$  in terms of  $\delta P_0$ . As a function of  $z$ , the denominator in Eq. (B46) has a zero at  $z = z(\omega)$ , obtainable from a knowledge of the fixed point  $P(\omega)$ , Eq. (B32). In the neighborhood of

$\omega = i$ ,  $z(\omega)$  is of  $O(1 + i\omega)$ , which is small, and so clearly lies inside the unit circle. In addition, there is a contribution from the pole at  $z = 0$  from the  $dz/z$  in Eq. (B47). However,  $\delta \mu(z)$  will be analytic inside the unit circle. Adding the contributions from the two poles and simplifying, we obtain

$$\delta \mu[z(\omega)] = - \frac{(1 + i\omega) \delta P_0(\omega)}{i\omega z} \quad (\text{B48})$$

giving an explicit expression by inverting  $z(\omega)$  to get  $\omega(z)$ . Since the generating functional  $P(\omega)$  and  $\delta P_0(\omega)$  should be well behaved for small  $z$  and in the neighborhood of  $\omega = i$  (since  $P(\omega = i) = \int d\Delta P(\Delta) \exp[-\Delta]$ ), we obtain the solution  $\delta \mu(z)$  by analytic continuation of Eq. (B48); in particular, we use the analytic continuation of the function  $\omega(z)$  from  $\omega(z = 0) = i$ . It is then possible to obtain  $\delta \mu_m$  from Eq. (B48) by contour integration.

From Eqs. (B32) and (B46),  $z(\omega)$  is given by

$$\begin{aligned} z(\omega) &= (1 + i\omega) / \left[ 1 + i\omega \right. \\ &\left. - i\omega \sqrt{(1 - 2g - ig\omega)/(1 - ig\omega)} \right]. \end{aligned} \quad (\text{B49})$$

We choose the branch cut in the denominator to extend along the negative imaginary axis, to satisfy the analyticity requirements. From Eq. (B49),  $z(\omega) = 1$  at  $\omega = 0$ , and at the origin of the branch cut  $\omega = -i(1 - 2g)/g$ . These two points approach each other as  $g \rightarrow g_T = \frac{1}{2}$ . For  $g < g_T$ , moving along the negative imaginary axis in  $\omega$ ,  $z(\omega)$  is real and has a maximum between these two points, at  $\omega_c = -O(\epsilon)i$ . At this point,  $z(\omega_c) \equiv z_c = 1 + O(\epsilon^{3/2})$ . This is a simple quadratic maximum, so that in its neighborhood,  $\omega(z)$  has a square-root branch cut:

$$\omega(z) = \omega_c + iC\epsilon^{1/4} \sqrt{z_c - z}. \quad (\text{B50})$$

(The strength of the branch cut has been fixed by the requirement that at  $z = 1$ ,  $\omega = 0$ .)

The initial perturbation  $\delta P_0(\omega)$  can be chosen to be well behaved around  $\omega = \omega_c$ , so that the branch cut in Eq. (B50) will carry over into the contour integration needed to find  $\delta \mu_m$  from Eq. (B48). The apparent pole at  $\omega = 0$  in Eq. (B48) is cancelled by the numerator: since  $P$  is a normalized probability distribution,  $\delta P_0(\omega = 0)$  is zero, and if we restrict ourselves to perturbations  $\delta P_0(\Delta)$  for which the first moment exists, the pole is cancelled. Other singularities in  $\delta P_0(\omega)$  will occur further out in  $z$  as compared to the branch cut of Eq. (B50), provided we only consider perturbations that do not decay more slowly at large  $\Delta$  than  $P(\Delta)$ . In particular, one can verify these properties for the simple case,  $\delta P_0(\omega) \sim i\omega P(\omega)$ , which corresponds to adding fluid randomly to a small fraction of the sites. From Eq. (B50), the asymptotic form of  $\delta \mu_m$  for large  $m$  is then

$$\delta \mu_m \sim \frac{\epsilon^{1/4}}{m^{3/2}} \exp \left[ -4(2\epsilon/3)^{3/2} m \right]. \quad (\text{B51})$$

The decay length for  $\delta \mu_m$  is thus  $\sim \epsilon^{-3/2}$ . We expect that  $\delta \mu_m$  will decay over a length of the order of the

characteristic cluster size (i.e., the correlation length), so that Eq. (B51) implies  $\xi \sim \epsilon^{-3/2}$ , i.e.,

$$\nu = \frac{3}{2}. \quad (\text{B52})$$

Together with Eq. (B41), this gives us

$$d_f = 4/3. \quad (\text{B53})$$

From Eqs. (B42) and (B49), we have for the fraction of sites in large clusters, the exponent

$$\kappa = 2/3. \quad (\text{B54})$$

At threshold, the branch cut in  $z$  occurs at  $z = 1$ . Nearby,  $z(\omega) = 1 + O([i\omega]^{3/2})$ , so that  $\omega = iO([z - 1]^{2/3})$ , and hence

$$\delta\mu_m \sim \frac{1}{m^{5/3}}. \quad (\text{B55})$$

Note that this scales in the same way as Eq. (B51). Physically,  $\delta\mu_m$  is the probability of a small amount of extra fluid added to some random site in the lattice flowing downhill for  $m$  rows before it reaches the end of a cluster.<sup>42</sup> This scales like the probability of being in a cluster of length  $m$ , so that from Eq. (3.1),  $\delta\mu_m \sim m^{-(1+\kappa)}\Phi(m/\xi)$ . The conjectured scaling form is thus in agreement with Eqs. (B51), (B54), and (B55). In principle, one could calculate the full scaling function, although we have not done this.

#### 4. Breakdown of finite size scaling for $d = 1$

A similar calculation of the effects of a perturbation can be performed much more easily for  $d = 1$ . The difference is that  $dP(\omega)/d\omega|_{\omega=0}$  is  $O(1/\epsilon)$ , so that there is an additional factor of  $1/\epsilon$  in  $\delta\mu_m$ , apart from the singularity from the branch cut. We obtain

$$\delta\mu_m \sim \frac{1}{m^{3/2}\epsilon} \exp[-\epsilon^2 m]. \quad (\text{B56})$$

This yields  $\nu = 2$ , in agreement with Eq. (B28). From the requirement that  $\delta\mu_m$  should scale as  $m^{-(1+\kappa)}$ , we find  $\kappa = 0$ , in agreement with Eq. (B29).

As mentioned after Eq. (3.24), the finite size scaling is anomalous for  $d = 1$ . On substituting  $d = d_f = 1$  and  $\kappa = 0$  into the conjectured scaling law Eq. (3.24b), we obtain the result that the mean number of clusters connecting the top to the bottom of a region of length  $L$  that is part of an infinite system is independent of  $L$  at the critical point. However the probability  $p_c$  of a *finite system* of length  $L$  being connected from top to bottom scales differently in one dimension:  $p_c(L, F = F_T)$  is the probability that  $\sum_{i=0}^m a_i$  is greater than zero for all  $0 \leq m \leq L$ , since this is required for fluid to pour out of the  $m$ th row to the  $(m + 1)$ th for all  $m$ . At threshold, the first moment of  $A(a)$  is zero, so that the  $a_i$ 's represent the steps of an unbiased random walker. The probability  $p_c(L, F_T)$  is then the probability that a random walker does not return to its starting point before  $L$  time steps,

which is  $\sim 1/\sqrt{L}$ .

The source of this difference in scaling can be understood easily. For finite size systems, the sites in the top layer do not receive any fluid from above. The distribution of fluid in these sites,  $P_0(\omega)$ , is not the fixed point  $P(\omega)$ , but  $A(\omega)$ . The perturbation in the distribution of fluid in these sites,  $\delta P_0(\omega)$ , should be taken to be  $i\omega A(\omega)$  rather than the  $i\omega P(\omega)$  that we have used to derive Eq. (B56). This removes a factor of  $1/\epsilon$  which, since  $\nu = 2$ , yields an extra factor of  $1/\sqrt{L}$  in the finite size scaling. In mean-field theory, where the quadratic nature of the equation for  $P$  restricts us to small perturbations  $\delta P$ , it is not possible to replace the distribution of fluid at the top of the lattice by  $A(\omega)$  (as we have done here for  $d = 1$ ) and still obtain an exact solution. However, we can approximately estimate finite size effects by replacing  $P(\omega)$  at the top by  $P(\omega) + \lambda[A(\omega) - P(\omega)]$ , which corresponds to randomly cutting off the inputs to a fraction  $\lambda$  of the sites in the top row, and examining the behavior as a function of  $\lambda$  for small  $\lambda$ . Adding fluid to all the sites at the top is equivalent to  $\delta P_0(\omega) = i\omega \left\{ P(\omega) + \lambda[A(\omega) - P(\omega)] \right\}$ . Unlike the case for  $d = 1$ ,  $dP(\omega)/d\omega|_{\omega=0}$  is not singular near the critical point, so that the  $\lambda$ -dependent part scales in the same way as Eq. (B51). Thus the scaling of finite size quantities is *not* anomalous in mean-field theory. We expect this to also be the case for all dimensions  $d$  greater than 1, since except in one dimension there are many sites in the top row.

#### 5. Generalizations

There are two major simplifications we have made in deriving the solutions in the previous subsections: (i) the special form of the distribution  $A(a)$  we have chosen, and (ii) the restriction to no more than two inputs per site for the mean-field solution ( $c_r = 0$  for  $r > 2$ ). It is important to ask if the form of the singularities we have obtained will be modified, if either of these two is changed.

We first consider whether other choices for  $A(a)$ , also with exponential tails for  $a < 0$ , but with different forms for  $a > 0$ , would yield the same exponents. While for the particular choice of  $A(a)$  that we made it was possible to obtain all the singularities in the complex  $\omega$  plane, since the equations we had to solve were all effectively quadratic, this is not the case for a more general distribution. For instance, for the distribution of Eq. (3.12), corresponding to  $A(\omega) = \exp[iF\omega]/(1 + i\omega)$ , where the tuning parameter  $F$  shifts the entire distribution  $A(a)$  to the right (a more accurate representation of the effect of increasing the tilt), Eq. (B31) gives a transcendental expression for  $P(\omega)$ . However, it is only the behavior in the region around the origin,  $\omega = 0$ , which is the *same* for all these distributions, that determines the critical behavior. The only way in which other singularities could be important is if, for some particular form of  $A(\omega)$ , the singularity at  $\omega = 0$  that we have considered were to be "preempted" by one at  $\omega \neq 0$  that approaches the real axis earlier. [Singularities with a more negative value for

$\text{Im}(\omega)$  give rise to corrections that decay rapidly at large  $\Delta$  and do not change the critical behavior.] However, if a singularity at  $\omega \neq 0$  were to dominate, it would lead to oscillations in  $P(\Delta)$  at large  $\Delta$ . This is not possible for a physical probability distribution  $P(\Delta)$  which must satisfy the condition  $P(\Delta) \geq 0$ . Reasonable distributions  $A(a)$ , by other singularities in  $\mu(y)$ , single point where all quantities distributions will be the same. For a nonexponential choice of  $A(a)$ , we have not been able to solve Eq. (B7). However, we believe that, so long as we restrict consideration to distributions which decay away rapidly for large positive  $a$ , the universal results will not change, though power-law tails in  $A(a)$  could certainly lead to modified critical behavior.

If we allow multiple inputs to a site, Eq. (B14) is no longer quadratic in  $P(\omega)$  and, in general, we cannot obtain a closed form expression for the solution. However, we can still obtain information perturbatively. Expanding around  $\omega = 0$  and  $P = A = 1$ , with  $P(\omega) = 1 + p(\omega)$ , Eq. (B14) becomes

$$1 + p = A(\omega) \left\{ \left[ \sum c_r \right] + \left[ \sum r c_r \right] p + \frac{1}{2} \left[ \sum r(r-1) c_r \right] p^2 + \dots \right\} + \frac{i\mu\omega}{1+i\omega}. \quad (\text{B57})$$

Any choice of  $c_r$ 's has to satisfy the constraints  $\sum c_r = 1$ , and  $\sum r c_r = 1$ . To lowest order, Eq. (B57) is

$$0 = \frac{1}{2} \left[ \sum r(r-1) c_r \right] p^2 + [A'(\omega=0) + i\mu] \omega \quad (\text{B58})$$

with  $A'(\omega) = dA(\omega)/d\omega$ . Thus as before,  $p$  has a branch cut at  $\omega = 0$ , unless  $\mu$  is adjusted to be equal to  $iA'(0)$  (or  $c_r = \delta_{r,1}$ , i.e., the one-dimensional case). With this choice of  $\mu$ , the lowest-order terms in Eq. (B57) are

$$0 = \frac{1}{2} \left[ \sum r(r-1) c_r \right] p^2 + A'(0) \omega p + [iA'(0) + A''(0)] \omega^2. \quad (\text{B59})$$

Thus  $p = O(\omega)$ . There are  $O(\omega^3)$  corrections to the right-hand side of Eq. (B59). As long as the quadratic part of this equation is of the form  $\sim (p - \lambda_1 \omega)(p - \lambda_2 \omega)$ , the change in  $p$  that is needed to cancel these corrections is  $O(\omega^3)/(\lambda_1 - \lambda_2)$ . For some value of  $A'(0)$  and  $A''(0)$ , which depends on the value of the  $c_r$ 's, Eq. (B59) will have a double root for  $p$ , and then takes the form  $(p - \lambda\omega)^2 = 0$ . The  $O(\omega^3)$  corrections to Eq. (B59) then imply that  $p = \lambda\omega + O(\omega^{3/2})$ , so that we again have a singularity at  $\omega = 0$ , of the same  $\omega^{3/2}$  form as Eq. (B32) at  $g = g_T$ , and hence a similar resulting power-law distribution for  $P(\Delta)$ . A complete analysis would require us to obtain the cluster distribution functions. For a general choice of  $c_r$ 's, we have not been able to obtain an expression for these. In fact, it is not even clear how to choose between the two roots for  $\delta P$  within the perturbative approach we are considering here. However, with the same assumption that we made for general forms for  $A(a)$ , about there being a single point where all quantities diverge, the scaling and other universal properties are likewise expected to be independent of the choice of

the  $c_r$ 's. We thus expect that the mean-field results are universal for well-behaved distributions  $A(a)$  and  $c_r$ .

### APPENDIX C: MEAN-FIELD THEORY ABOVE THRESHOLD

In this appendix, we analyze a mean-field version of our lattice model *above* threshold, expressed in terms of the currents rather than the driving force  $F$ . This approach was discussed briefly in Sec. IV.

As in Appendix B, in mean-field theory each site in a given level is equally likely to be connected to any of the sites in the next level down, so that the concept of transverse distance is irrelevant, and again we expect independence from site to site within one level in the large system limit.

In steady state, the sum of all the currents feeding into any site has to be equal to the sum of all the output currents. Close to threshold, most sites will have current flowing out from them only over the lowest emerging barrier, so that there is a single outgoing current,  $J_i (\geq 0)$ , associated with each site. But, there will be corrections to this due to the infrequent splits in the rivers. It is convenient to consider the process of moving from one level to the next one downhill in two stages: in the first stage, rivers are only allowed to join with each other, while in the next stage, the appropriate rivers are allowed to split.

At the first stage, where there are no river splits, each site has only one outlet from it. As in Appendix B, we simplify the problem by the restriction that each site receives inputs from zero, one, or two sites in the previous row, with probabilities  $1/4$ ,  $1/2$ , and  $1/4$ , respectively. Since the current emerging from a site,  $J_i$ , has to be the sum of the incoming currents, in the *absence of splits* the probability distribution of currents  $P(J)$  evolves from one row to the next one down as

$$P'(J) = \frac{1}{4} \delta(J) + \frac{1}{2} P(J) + \frac{1}{4} \int_0^J dJ_1 P(J_1) P(J - J_1) \quad (\text{C1})$$

(where we have dropped the level indices of Appendix B). By Laplace transforming Eq. (C1), it is easy to see that the steady state distribution  $P(J)$  in the absence of splits is  $P(J) = \delta(J)$ , (with an infinitesimal weight out at infinite  $J$  to satisfy current conservation), which is what is expected, because of the tree structure in the absence of splits.

Equation (C1) now has to be modified by the effect of splits. At a site where the flow splits, current is output to *two* sites in the next row instead of one. Close to threshold, the rivers are very sparse, and we can assume that the secondary site that is fed into would have otherwise had zero current flowing through it. Thus the effect of a river split is to eliminate two sites in the next row, with outgoing currents  $J = 0$  and  $J = J_i$ , and replace them with two sites with currents  $J_i^a$  and  $J_i^b$ . The equations that determine  $J_i^a$  and  $J_i^b$  are

$$J_i = J_i^a + J_i^b, \quad (\text{C2a})$$

from current conservation, and

$$\delta b_i = (J_i^a)^{1/\beta_0} - (J_i^b)^{1/\beta_0}, \quad (\text{C2b})$$

where  $\delta b_i$  is the difference in the heights of the lowest and the next lowest barriers out of the site  $i$ , and  $\beta_0$  is the exponent in the local constitutive equation, defined in Eq. (2.3).

For arbitrary  $\beta_0$ , we are limited to the scaling arguments discussed in Sec. IV; with a probability distribution for  $\delta b$  that is uniform at small  $\delta b$  (or varies as some

power of  $\delta b$ ), both Eqs. (C2) are homogeneous in the  $J$ 's, and so one can rescale currents in an ensemble of systems with different barrier heights.

For the case of  $\beta_0 = 1$ , however, one can readily solve the resulting equations. Equations (C2) are equivalent to

$$J_i = 2J_i^a - \delta b_i = 2J_i^b + \delta b_i. \quad (\text{C3})$$

With  $Q(\delta b)$  the distribution of  $\delta b$ , Eq. (C1) is modified to

$$\begin{aligned} P'(J) = & \frac{1}{4}\delta(0) + \frac{1}{2}P(J) + \frac{1}{4}\int_0^J dJ_1 P(J_1)P(J-J_1) \\ & + \left\{ 2\int_0^\infty d\delta b Q(\delta b)P(2J+\delta b) + 2\int_0^J d\delta b Q(\delta b)P(2J-\delta b) \right. \\ & \left. - P(J)\int_0^J d\delta b Q(\delta b) - \delta(J)\int_0^\infty dJ P(J)\int_0^\infty d\delta b Q(\delta b) \right\}, \end{aligned} \quad (\text{C4})$$

where the terms in the brackets arise from the elimination of two sites with  $J = 0$  and  $J = J_i$  in favor of  $J_i^a$  and  $J_i^b$  whenever  $\delta b_i < J_i$ .

It is straightforward to verify that both Eqs. (C1) and (C4) satisfy the conservation laws,  $\int dJ P'(J) = 1$  if  $\int dJ P(J) = 1$ , and  $\int dJ J P'(J) = \int dJ J P(J)$ . In the critical regime, we guess a form for  $P(J)$ , which is close to that in the absence of splits

$$P(J) = (1-c)\delta(J) + \frac{1}{\alpha}\exp[-J/\alpha]. \quad (\text{C5})$$

For small  $c$ , this has most of its weight at  $J = 0$ , and has negligible strength for  $J > O(c)$ . Since we are interested in the limit,  $c \rightarrow 0$ , we only need the form of  $Q(\delta b)$  for small  $\delta b$ , where we may treat it as a uniform distribution,  $Q(\delta b) = Q_0$ . Substituting this and Eq. (C5) in Eq. (C4), we indeed find a fixed point distribution  $P(J)$  of the form Eq. (C5) with  $\alpha = 1/4Q_0$ . The mean density of rivers  $\phi_R$  is given by the weight of  $P(J)$  away from  $J = 0$ , so that

$$\phi_R = c, \quad (\text{C6})$$

while the mean current carried is the first moment of  $P(J)$ , which is

$$\bar{J} \propto c^2. \quad (\text{C7})$$

Thus we have  $\phi_R \sim \sqrt{\bar{J}}$ , which agrees with the conjecture Eq. (4.19) for the case  $\beta_0 = 1$ . The probability of river splits, which is the inverse of the correlation length  $\xi'$ , can be seen from Eqs. (C4) and (C5) to be  $O(c)$ . Hence

$$\xi' \sim \bar{J}^{-1/2}. \quad (\text{C8})$$

We now consider the stability of this distribution to perturbations. Since the first moment of the distribution is conserved under Eq. (C4) we consider a change  $\delta P(J)$  to the fixed point distribution  $P(J)$ , with vanishing zeroth

and first moments of  $\delta P$ . Linearizing around Eq. (C4), we obtain (after substituting  $Q = Q_0$ )

$$\begin{aligned} \delta P'(J) = & \frac{1}{2}\delta P(J) + \frac{1}{2}\int_0^J dJ_1 \delta P(J_1)P(J-J_1) \\ & + \left\{ 2\int_J^\infty dJ_1 \delta P(J_1) - J\delta P(J) \right\} Q_0. \end{aligned} \quad (\text{C9})$$

We can rescale all currents to set  $\alpha$  in Eq. (C5) to 1, which corresponds to  $Q_0 = 1/4$ . Equation (C9) then reduces to

$$\begin{aligned} \delta P'(J) = & \left(1 - \frac{c}{2}\right)\delta P(J) \\ & + \frac{1}{2}\int_0^J \delta P(J_1) \exp[(J_1 - J)/c] dJ_1 \\ & + \frac{1}{2}\int_J^\infty dJ_1 \delta P(J_1) - \frac{1}{4}J\delta P(J). \end{aligned} \quad (\text{C10})$$

We look for an eigenvalue solution:  $\delta P'(J) = \lambda\delta P(J)$ . Upon Laplace transforming this equation,  $\delta P(u) = \int_0^\infty dJ \delta P(J) \exp[-uJ]$ , we have

$$\left[ 2 - 2\lambda - c + \frac{c}{1+cu} - \frac{1}{u} \right] \delta P(u) + \frac{1}{2} \frac{d\delta P(u)}{du} = 0, \quad (\text{C11})$$

where we have used the fact that the zeroth moment of  $\delta P$ ,  $\delta P(u = 0)$ , is zero. This can be integrated to give

$$\delta P(u) = \frac{u^2}{(1+cu)^2} \exp[-2(2-2\lambda-c)u] \quad (\text{C12})$$

(with  $d\delta P(u)/du|_{u=0} = 0$ , as required by current conservation). If  $2 - 2\lambda - c$  were less than zero, transforming back to  $\delta P(J)$  would produce a nonzero weight for  $J < 0$ , which would be unphysical. Therefore the eigenvalue spectrum of perturbations to the fixed point distribution is bounded above by  $1 - c/2$ . This implies that

the effect of perturbations to the distribution decay over a length  $\sim 1/c$ , implying that

$$l_{\text{decay}} \sim \xi' \sim (\bar{J})^{-1/2}, \quad (\text{C13})$$

consistent with the results for  $\bar{J}$  and the distance between splits as well as the conjectured form Eq. (4.20b). Strictly speaking, the analysis of perturbations should be carried out by a fuller analysis of the non-self-adjoint linear operator in Eq. (C4) as was done in Appendix B below threshold. However, if in that case we had done a simple search for eigenvalues as done here, the correct scaling of the correlation length would have been obtained. We thus trust that a fuller analysis here would again yield the same scaling law Eq. (C13).

In order to characterize the behavior above threshold more fully, obtaining the distribution of the fluid as well as the current distribution, it would be necessary to study the time evolution of the system instead of just considering the steady state. With the same distribution of

currents, there are many different steady state solutions that are possible, since pouring extra fluid into unsaturated sites does not destroy the steady state. The steady state solution that the system actually reaches is determined by the initial condition: that we start with fluid randomly distributed in the sites of the lattice, and then tilt the system. Unfortunately, with time-dependent distributions,  $P(\delta, J, t)$ , we have not been able to obtain a mean-field equation for the evolution of the system in terms of the distribution  $P$ . This is because, at any time  $t$ , more fluid moves out to neighboring sites from sites which themselves have a large amount of fluid in them. This “diffusion” of the fluid results in nontrivial correlations between  $\delta$  (and therefore  $J$ ) for the different sites; thus even if we *start* with the fluid distribution in the different sites being uncorrelated, this is no longer true after the system evolves. Note however that this does not create any difficulties for a *numerical* simulation of the lattice (with periodic boundary conditions connecting the top to the bottom). We leave this and further analytical work for future study.

- 
- <sup>1</sup> A.I. Larkin and Yu. N. Ovchinnikov, *J. Low Temp. Phys.* **34**, 409 (1979).
- <sup>2</sup> M.V. Feigel'man and V.M. Vinokur, *Phys. Rev. B* **41**, 8986 (1990).
- <sup>3</sup> A. Brass, H.J. Jensen, and A.J. Berlinsky, *Phys. Rev. B* **39**, 102 (1989).
- <sup>4</sup> D.S. Fisher, M.P.A. Fisher, and D.A. Huse, *Phys. Rev. B* **43**, 130 (1991), and references therein.
- <sup>5</sup> M.A. Rubio, C. Edwards, A. Dougherty, and J.P. Gollub, *Phys. Rev. Lett.* **63**, 1685 (1989); V.K. Horvath, F. Family, and T. Vicsek, *Phys. Rev. Lett.* **65**, 1388 (1990); M.A. Rubio, A. Dougherty, and J.P. Gollub, *ibid.* **65**, 1389 (1990); V.K. Horvath, F. Family, and T. Vicsek, *ibid.* **67**, 3207 (1991); S. He, G.L.M.K.S. Kahanda, and P-Z. Wong, *ibid.* **69**, 3731 (1992).
- <sup>6</sup> R. Lenormand and C. Zaccaro, *Phys. Rev. Lett.* **54**, 2226 (1985).
- <sup>7</sup> M. Cieplak and M.O. Robbins, *Phys. Rev. Lett.* **60**, 2042 (1988); *Phys. Rev. B* **41**, 11508 (1990); N. Martys, M. Cieplak, and M.O. Robbins, *Phys. Rev. Lett.* **66**, 1058 (1991); N. Martys, M.O. Robbins, and M. Cieplak, *Phys. Rev. B* **44**, 12294 (1991); B. Koiller, H. Ji, and M.O. Robbins, *ibid.* **45**, 7762 (1992).
- <sup>8</sup> K.J. Måløy, J. Feder, and T. Jøssang, *Phys. Rev. Lett.* **55**, 2688 (1985); J.D. Chen and D. Wilkinson, *ibid.* **55**, 1892 (1985); K.J. Måløy, F. Boger, J. Feder, T. Jøssang, and P. Meakin, *Phys. Rev. A* **36**, 318 (1987); J.P. Stokes, D.A. Weitz, J.P. Gollub, A. Dougherty, M.O. Robbins, P.M. Chaikin, and H.M. Lindsay, *Phys. Rev. Lett.* **57**, 1718 (1986).
- <sup>9</sup> For a collection of work on CDW's see *Charge Density Waves in Solids*, edited by Gy. Hutiray and J. Sólyom, Lecture Notes in Physics Vol. 217 (Springer-Verlag, Berlin, 1984); and *Charge Density Waves in Solids*, edited by L.P. Gorkov and G. Grüner (Elsevier, Amsterdam, 1989).
- <sup>10</sup> D.S. Fisher, *Phys. Rev. B* **31**, 1396 (1985). Here and in some other references, the exponent  $\beta$  is called  $\zeta$ .
- <sup>11</sup> L. Niemeyer, L. Pietronero, and H.J. Wiesmann, *Phys. Rev. Lett.* **52**, 1033 (1984); P. Meakin, G. Li, L.M. Sander, E. Louis, and F. Guinea, *J. Phys. A* **22**, 1393 (1989).
- <sup>12</sup> A.A. Middleton and D.S. Fisher, *Phys. Rev. Lett.* **66**, 92 (1991), and references therein; *Phys. Rev. B* **47**, 3530 (1993); O. Narayan and D.S. Fisher, *Phys. Rev. Lett.* **68**, 3615 (1992); *Phys. Rev. B* **46**, 11520 (1992); C.R. Myers and J.P. Sethna, *ibid.* **47** 11171 (1993).
- <sup>13</sup> However, S.N. Coppersmith, *Phys. Rev. Lett.* **65**, 1044 (1990), has shown that on sufficiently long length scales, the elastic theory always breaks down.
- <sup>14</sup> For a review of scaling properties of percolation, see D. Stauffer, *Phys. Rep.* **54**, 1 (1979).
- <sup>15</sup> For a review of various types of percolation, see G. Grimmett, *Percolation* (Springer-Verlag, New York, 1989).
- <sup>16</sup> D. Wilkinson and J. Willemsen, *J. Phys. A* **16**, 3365 (1983); D. Wilkinson and M. Barsony, *ibid.* **17**, L129 (1984); R. Chandler, J. Koplik, K. Lerman, and J.F. Willemsen, *J. Fluid. Mech.* **119**, 249 (1982).
- <sup>17</sup> S.P. Obukhov, *Physica A* **101**, 145 (1980); S. Redner and Z.R. Yang, *J. Phys. A* **15**, L177 (1982); A.R. Day and T.C. Lubensky, *ibid.* **15**, L285 (1982).
- <sup>18</sup> The *characteristic size* of the connected clusters is not the same as the *mean size*. The concept of characteristic size is made precise in the scaling analysis discussed later.
- <sup>19</sup> However, in mean field, and for dimensions greater than three, there are *correlations* in the current over much larger transverse distances than the distances over which the current is inhomogeneous, so that  $\xi_{\perp}$  is actually bigger.
- <sup>20</sup> The exponent  $\beta$  is often called  $\zeta$  in the CDW literature.
- <sup>21</sup> The *existence* of a steady state solution does not imply that it is appropriate; the correct solution is one that starts with the fluid confined in the lakes before the tilt is applied. the current flowing out of the bottom of the system with this initial condition could in principle be intermittent. In Appendix A it is shown that this is not the case close to threshold; in fact, with a fluid model, one might expect any intermittency near the top of the system to get smeared out as the current moves downhill, so that, apart from boundary effects, the steady state solution should be applicable even away from threshold.

- <sup>22</sup> S. Feng, B.I. Halperin, and P.N. Sen, *Phys. Rev. B* **35**, 197 (1987).
- <sup>23</sup> Distributions and their Fourier transforms are denoted by the same symbols, and are distinguished by their arguments.
- <sup>24</sup> J.T. Chayes, L. Chayes, D.S. Fisher, and T. Spencer, *Phys. Rev. Lett.* **57**, 2999 (1986).
- <sup>25</sup> Strictly speaking, since the lattice model should be viewed as the continuum system with the rivers connecting the lakes ignored, these “flowing river sites” are more appropriately lakes which are connected by the flowing rivers and through which the current flows.
- <sup>26</sup> This is only correct if all the depths  $\delta_i$  scale homogeneously under a change in  $f$ . We shall address this issue later.
- <sup>27</sup> The mean separation,  $w$ , is dominated by the *true* splits in the rivers, since the probability of a branch surviving for a length  $l$  is proportional to  $l^{(d-3)/2}$ , so that the probability of intersecting a branch of length  $l$  in an arbitrary row of the lattice is  $\sim l^{(d-1)/2}$ , which is dominated by long-lasting branches, i.e., of length  $\sim \xi^l$ , for any  $d > 1$ .
- <sup>28</sup> Although the equality between bifurcations and recombinations in any row is only statistical in nature in the real system, and not exact, we expect this will not matter for sufficiently large systems. The change we have made is similar to replacing a grand canonical ensemble with a canonical one.
- <sup>29</sup> A similar feature is seen in first-order phase transitions in random systems (Ref. 30), where the rounding in the critical temperature in any finite size system of size  $L^d$  is  $\Delta T_c \sim L^{-d}$ , i.e.,  $L \sim (\Delta T_c)^{-1/d}$ , yielding an apparent  $\nu = 1/d < 2/d$ .
- <sup>30</sup> M.N. Barber, in *Phase Transitions and Critical Phenomena*, edited by C. Domb and J.L. Lebowitz (Academic Press, London 1983), Vol. 8.
- <sup>31</sup> For a discussion of the effect of noise at the boundary inputs with discrete transport carriers, see G. Grinstein, T. Hwa, and H.J. Jensen, *Phys. Rev. A* **45**, R559 (1992).
- <sup>32</sup> In CDW’s, the “boundary” voltage drop is actually spread across the entire system, as shown in S. Ramakrishna, M.P. Maher, V. Ambegaokar, and U. Eckern, *Phys. Rev. Lett.* **68**, 2066 (1991). This does not affect our argument here.
- <sup>33</sup> P. Bak, C. Tang, and K. Wiesenfeld, *Phys. Rev. Lett.* **59**, 381 (1987); P. Bak and K. Chen, in *Nonlinear Structure in Physical Systems—Pattern Formation, Chaos and Waves*, edited by L. Lam and H.C. Morris (Springer-Verlag, Berlin, 1990).
- <sup>34</sup> S. Tyč and B.I. Halperin, *Phys. Rev. B* **39**, 877 (1989).
- <sup>35</sup> J.T. Chayes, L. Chayes, and C.M. Newman, *Comm. Math. Phys.* **101**, 383 (1985).
- <sup>36</sup> L. deArcangelis and H.J. Herrmann, *J. Phys. A* **23**, L923 (1990).
- <sup>37</sup> For isotropic percolation with bond strengths weakening with distance, it is found to be necessary to use multifractal scaling forms to describe the shape of the invaded cluster.
- <sup>38</sup> S. Kramer and M. Marder, *Phys. Rev. Lett.* **68**, 205 (1992).
- <sup>39</sup> H. Takayasu, *Phys. Rev. Lett.* **63**, 2563 (1990); G. Huber, *Physica A* **170**, 463 (1991).
- <sup>40</sup> W.J. Yeh and Y.H. Kao, *Phys. Rev. Lett.* **53**, 1590 (1984).
- <sup>41</sup> R. Seshadri and R.M. Westervelt, *Phys. Rev. Lett.* **66**, 2774 (1991); **70**, 234 (1993).
- <sup>42</sup> Strictly speaking,  $\delta\mu_m$  is the probability that a small amount of fluid reaches the bottom of a cluster  $m$  rows down and *extends* the cluster; the probability of extending a cluster is not singular, at least for the exponential distributions  $A(a)$  considered here.